AN *IN VITRO* MODEL FOR LYSOSOMAL STORAGE DISEASES USING ASPARTYLGLUCOSAMINURIA PATIENT CELLS

Master´s Thesis
University of Turku
MSc Degree Programme in
Biomedical Sciences
Drug Discovery and Development
4/2020

Maria Kjellman

Supervisors
Riikka Äänismaa, PhD
Senior Scientist
Therapy Area Rare Diseases
Orion Corporation Orion Pharma

Jarkko Venäläinen, PhD
Principal Scientist
Therapy Area Rare Diseases
Orion Corporation Orion Pharma

Ullamari Pesonen, PhD
Professor of Pharmacology and Drug Development
Institute of Biomedicine
Faculty of Medicine
University of Turku

Pharmacology, Drug Development and Therapeutics

ABSTRACT
UNIVERSITY OF TURKU
Institute of Biomedicine, Faculty of Medicine

KJELLMAN, MARIA: An *In Vitro* Model for Lysosomal Storage Diseases Using Aspartylglucosaminuria Patient Cells
Master's Thesis, 73 pages
MSc Degree Programme in Biomedical Sciences
Drug Discovery and Development
April 2020

BACKGROUND Lysosomes are acidic organelles responsible for recycling of metabolic byproducts and cellular debris, and there are approximately 60 enzymes within lysosomes responsible for the recycling process. These enzymes can be malfunctional due to genetic mutations, which results in a lysosomal storage disease (LSD). One of these diseases is aspartylglucosaminuria (AGU) caused by an incorrectly folded aspartylglucosaminidase (AGA) enzyme, which results in a buildup of the substrate aspartylglucosamine. This enzymatic deficiency impairs the cellular function in both central nervous system (CNS) and periphery manifesting as an impaired physical and mental development.

UNMET MEDICAL NEED Currently, there are no curative or even symptom alleviating treatments available.

AIM The aim of this research was to establish a reliable *in vitro* model of LSD to enable repeatable experiments for drug development purposes.

MATERIALS AND METHODS Two cell types from an AGU patient and an age- and gender matched healthy individual were characterized. Characterization included enzyme activity and aspartylglucosamine concentration measurements, Western Blot studies and immunofluorescent stainings.

RESULTS The study showed significantly higher AGA activity in the healthy cells when compared to AGU cells, and the protein expression analysis revealed more of the precursor form of AGA in AGU cells. In line with this finding, aspartylglucosamine concentration was significantly higher in AGU cells. In addition, when AGU cells were treated with AGA, the enzyme activity could be replenished and aspartylglucosamine concentration normalized.

CONCLUSION Based on these measurements, an *in vitro* baseline for AGU and a healthy control is now established for future studies.

Key Words: Lysosomal storage diseases, aspartylglucosaminuria

Contents

2. Review of literature

2.1 Lysosomes

Lysosomes, first described in the 50s (De Duve *et al,* 1955), are small, acidic cell organelles of approximately 200-500 nm in size under normal conditions (Alberts *et al,* 2015). These acidic compartments have a resting [Ca^{2+}] of about 500 µM, which is 5000-fold higher compared with the cytosolic [Ca^{2+}] of 100 nM but over 10 000 times smaller than extracellular [Ca^{2+}]. From these intracellular storages, calcium is released through different calcium-channels, which are located within the lysosomal membrane (Christensen *et al,* 2002). Thus, lysosomes act as important intracellular calcium storages - which is the most common second messenger regulating various cellular functions from cellular growth and cell cycle to apoptosis. (Feng & Yang, 2016)

Lysosomes are rich in hydrolases that are responsible for the degradation of cellular biomaterial and different macromolecules, such as complex lipids and oligosaccharides, into reusable building blocks. After breakdown, these catabolites are transported into the cytosolic compartment and used by the cell in various metabolic reactions. (Bainton, 1981) In addition to the degrading function, lysosomes are regulators of receptor availability; they sense the need of nutrients, and control cholesterol homeostasis, exocytosis and cell death. Availability of nutrients is an essential factor in cellular homeostasis, which is regulated by activation of a crucial transcription factor, EB (TFEB). TFEB is described as the master regulator when it comes to genes regulating lysosomal function – indeed, TFEB is found to regulate at least 18 of the 23 lysosomal genes tested by Sardiello *et al,* 2009. Not only does TFEB control purely genes regulating lysosomal function, but TFEB also regulates genes within the CLEAR-network (Coordinated Lysosomal Expression and Regulation, Sardiello *et al,* 2009). Genes within this network are a direct downstream targets of TFEB, and encode for example proteins on the lysosomal membrane (*CLCN7, CLN3, TMEM55B*), proteins responsible of the acidification of lysosomes (*ATP6AP1, ATP6V0A1, ATP6V0B*) and proteins

that are not directly associated with lysosomes, but have a regulative function associated with the lysosomal biogenesis (*HPS1, NAGPA1, SUMF1*) (Palmieri *et al,* 2011). In addition to these functions, the TFEB and the downstream CLEAR-network regulate the transcription of genes *BECN1, GABARAP* and *SQSTM1,* which are mediators of autophagosome-formation (Palmieri *et al,* 2011; Kondratskyi *et al,* 2018). In conclusion of TFEB downstream targets, the master regulator of lysosomal function indeed orchestrates an elaborate system of lysosome-associated operations across the cell.

Activation of TFEB results in its translocation to nucleus, where it regulates the transcription of lysosomal genes resulting in, for example, activation of autophagy or lysosomal biogenesis. TFEB is activated through abnormal lysosomal function, such as extensive accumulation of cellular debris. Activation of TFEB was demonstrated by Sardiello *et al* in 2009, when they discovered that overexpression of TFEB resulted in a significant reduction in the amount of mutant huntingtin compared to a control cell line. Huntingtin protein is mutated and thus accumulating in Huntington's disease causing the pathology of the disease. In addition to Huntington's disease, activation of TFEB through lysosomal stress is present in other pathologies such as lysosomal storage diseases. In this group of diseases, the lysosomal stress is caused by abnormal lysosomal accumulation of macromolecules, which is the primary pathological process causing the disease.

Upstream from TFEB is its regulator, mechanistic target of rapamycin (mTOR). Under normal conditions, TFEB is kept in its phosphorylated, inactive form by mTOR residing on close proximity of lysosomes. This is crucial in order to respond to the changing circumstances within the lysosomes, for instance, to nutrient deprivation. If starvation, for example, occurs, mTOR separates from the lysosome resulting in the dephosphorylation of TFEB by calcineurin, activating the transcription factor followed by the relocation of TFEB to the nucleus and promotion of transcription of genes in response. (Bai *et al,* 2007) Although a very interesting signaling route connecting pathologies associated with lysosomes with pathologies affecting central nervous system (CNS), this literature review will not cover the specificities of the mTOR-TFEB route.

As the activation of lysosome biogenesis is initiated, there are several predecessors before the membrane coated organelles with acidic lumen are ready. Thus, there are several cytosolic organelles that resemble lysosomes and are partly responsible of similar tasks as lysosomes. However, lysosomes are distinguished from other acidic organelles by the absence of both cationdependent and cation-independent mannose 6-phosphate receptors (MPRs). (Eskelinen *et al,* 2003) Rather than lysosomes, MPRs are associated with early and late endosomes (EE and LE, respectively), which precede lysosomes in the maturation pathway of these organelles. These receptors can be used to distinguish the stages of lysosomes in their maturation process. (Sapmaz *et al,* 2019) The maturation process initiated by the mTOR-TFEB route includes several individual cellular organelles before the lysosomes reach their classical acidic lumen filled with catabolizing hydrolases.

2.1.1 Function and maturation

Lysosome maturation is a dynamic process in which the lumen of membrane-coated vesicular organelles acidifies towards the lysosomal pH. The predecessors of lysosomes have important functions in the cellular recycling process, and thus cannot be thought as passive predecessors but as active individual players. Thus, calling the acidification process a “maturation process” unnecessarily highlights lysosomes at the cost of the other players of this network, but since this thesis is focusing especially on lysosomes’ role in pathophysiology of lysosomal storage disease, the preceding steps are referred to as maturation process.

Lysosome biogenesis process starts from the Trans-Golgi-Network (TGN), where lysosomal hydrolases and membrane proteins are synthetized. From there, MPRs are responsible for transferring the hydrolases tagged with mannose 6phosphate (M6P) into endosomes, where MPRs dissociate from their cargo and are recycled back to the TGN (**Figure 1**). However, it must be kept in mind that transportation of the molecules is not limited to MPRs and

can be done with the help of e.g. low-density lipoprotein receptor-related protein, sortilin or LIMP2 (Hiesberger *et al,* 1998; Lefrancois *et al,* 2003; Reczek *et al,* 2007), depending on the transported protein in question and of the cell type. Thus, transportation of membrane proteins does not require binding of mannose 6-phosphate but can be reinforced by different proteins and accomplished either indirectly through plasma membrane or directly intracellularly. (Stoorvogel *et al*, 1991; Doray *et al*, 2002) Although several different alternative pathways for transportation to lysosomes have been described, M6P is still the main pathway of lysosomal transport and thus, will be looked into in more detail.

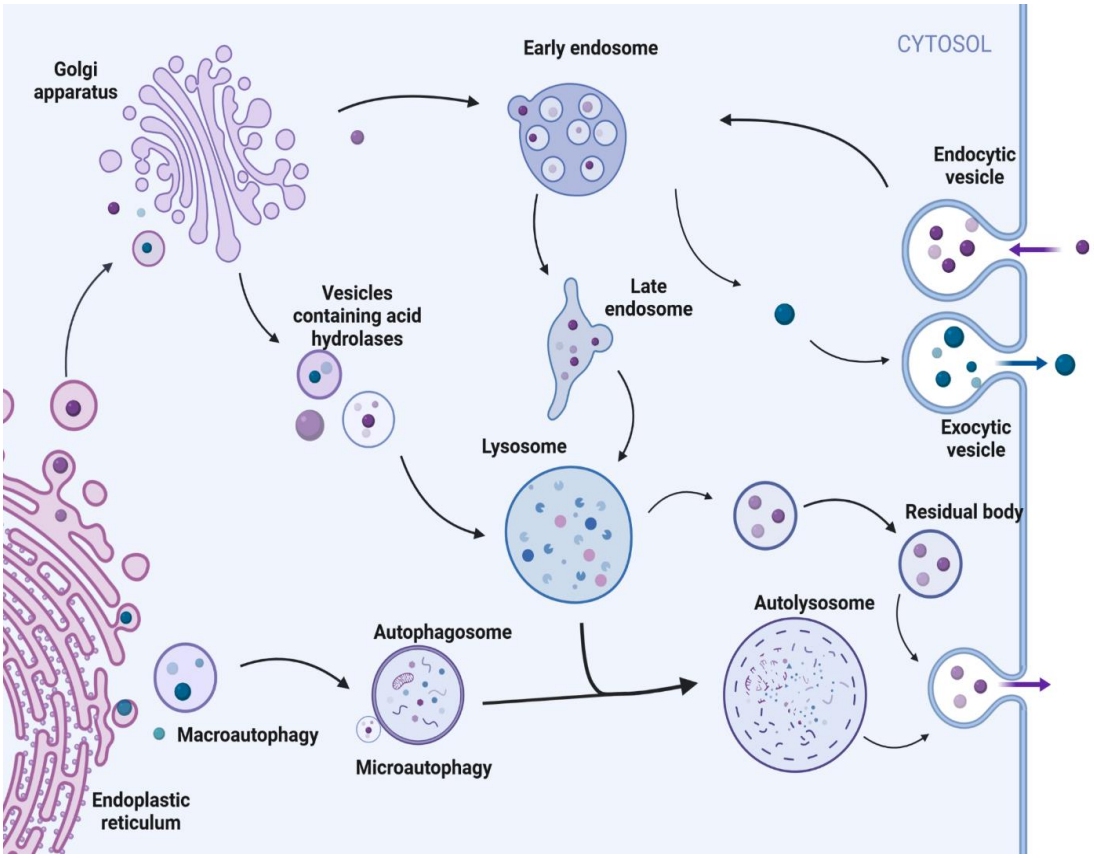

Figure 1. The route of the lysosomal proteins from Trans-Golgi Network (TGN) to lysosomes either directly from TGN with the help of mannose-6-phosphate (M6P) receptors or via the cellular membrane. The M6P tags help the proteins to be sorted correctly to lysosomes, but are themselves however cleaved by the acidification of the predecessors of lysosomes and recycled within the lysosomal protein synthesis process. Adapted from Schultz et al, 2011.

Transporting the lysosomal proteins to their intracellular destinations requires recognition signals. As briefly discussed in previous chapter, M6P and its receptor, MPR, are mainly responsible of the correct destination when transportation of lysosomal hydrolases and membrane proteins occurs. M6P is a unique marker for acid hydrolases destined to lysosomes, and this marker is added to the N-linked oligosaccharide chain that has a specific recognition signal, a specific group of nearby amino acids. (Alberts *et al,* 2015) Thus, not only a passive membrane protein used as a lysosome maturation indicator, M6Ps are heavily responsible of protein transportation to the lysosomes. (Reitman & Kornfeld, 1981) M6Ps are added to the lysosomal proteins during their production and maturation while they are transported from endoplasmic reticulum (ER) to TGN, after which the newly synthetized signal peptide is revealed in TGN. (Rohrer & Kornfeld, 2001) MPRs recognize M6Ps and bind to them on the inside of the transport vesicles. On the cellular side of the vesicles, MPRs bind to the transport vesicle assembly proteins. This ensures that the lysosomal hydrolases inside transport vesicles are packaged to the right vesicles with a correct intracellular destination. The hydrolases transit to cellular organelles preceding lysosomes, after which the M6P-receptors dislodge from the enzymes. This dislodging is induced by the drop in pH when they reach the predecessors of lysosomes with a pH of 6, which is approximately 0.5 lower than in the TGN. (Alberts *et al,* 2015) The MPRs are recycled back to TGN for their next cargo or relocated onto the cell surface, depending on their subtype.

MPRs can be divided into two different classes depending on their cationdependency when binding the M6Ps – to cation-dependent MPR (CD-MPR) and cation-independent MPR (CI-MPR). The CI-MPR can also be called insulin-like growth factor II -receptor (IGF-II-receptor) due to its ability to bind the IGFII as well. Only the cation-independent receptors relocate onto the cell surface in the recycling process of the receptors. These receptors relocating on the cell membrane are also responsible of capturing lysosomal hydrolases that have escaped the direct transportation route to the lysosomes and have instead been secreted to the extracellular space. There is, however, no harm in this extracellular detour, since the lysosomal hydrolases require an acidic

environment in order to be able to break down their substrate. Additionally, the cells have receptors for recapturing these circulating hydrolases. This relocation of the CI-MPRs onto the cellular surface provides the possibility to replenish the lysosomal enzyme depot with an extrinsically produced enzyme. This route is used in enzyme replacement therapy (ERT) where a functional enzyme is administered to the patients in order to restore the enzyme activity within the lysosomes. (Bajaj *et al,* 2019) Although seemingly a very straight-forward pathway to restore the enzyme activity to an appropriate state to alleviate the pathologies, there are problems with this approach, such as the poor brain penetration of the enzyme due to the protective function of blood brain barrier (BBB).

Although the M6P-route to lysosomes is addressed from the lysosomal point of view, the signal peptide is indeed cleaved before the cellular membrane-coated vesicle is classified as a “mature” lysosome. The first stage after leaving the TGN, are the EEs. As the lysosomal maturation progresses, EE is not only a passive middle stage in the lysosome maturation process, but rather an active recycling center for endocytosed extracellular material. Majority of the endocytosed material is actively recycled via the plasma membrane or excreted into extracellular space. (Kaur & Lakkaraju, 2018)

As the heavily regulated active recycling of cellular waste and metabolic byproducts continues, traffic between endosomes and TGN is constant. As the endosome matures, the recyclable material gathered from within the cell is transported back into TGN. In the meantime, lysosomal molecules are constantly delivered to the opposite direction, to the maturing late endosome. Late endosome is characterized by acidic hydrolases in the lumen and expression of lysosomal membrane proteins, e.g. Lysosome-associated Membrane Protein-1 (LAMP-1) (Bucci *et al*, 2000). Fusing with lysosomes, either fully or through “kiss-and-run” fusion, turns the late endosome either into an endolysosome or directly into a lysosome. These fusions require Ca^{2+} release, in a similar manner than lysosomal exocytosis when fusing with the cellular plasma membrane. Lysosomes have transmembrane calcium channels to fulfil this task, as mentioned before (Pryor *et al,* 2000; Christensen *et al,* 2002). Transformation between the maturation forms is not exact as the

maturation process is highly dynamic. However, a distinctive differentiation between the forms can be made in the descending pH value as the endosomes transform from early endosomes to late endosome and further into lysosomes through endolysosomes.

The pH drops from over 6 (EE), being 6-4.8 in LE and reaching as low as 4.5 in lysosomes. (Maxfield and Yamashiro, 1987) In addition to helping the hydrolysis process, acidic environment contributes to the trafficking of membrane molecules, pathogen inactivation and recycling process. Acidic environment and pH differences between the maturation stages of the organelles is maintained by ATP-dependent vacuolar proton pump (V-ATPase). V-APTases are transmembrane proteins that regulate the proton influx and they consist of different subunits. Thus, the activation stage of V-ATPases depends on the subunit activation, which changes through the maturation stages causing descending pH. (Trombetta *et al*, 2003; Lafourcade *et al*, 2008, Schwake *et al,* 2013)

Due to the highly acidic lumen of lysosomes and several degrading enzymes residing within the lysosomes, the lysosomal membrane is a crucial structure for protecting the cytosol from the hydrolases. In addition, the fusion with other organelles and cellular membrane requires regulatory proteins residing on the membrane of the vesicles. Often glycosylated, these membrane proteins are responsible for maintaining the lysosomal lumen intact and controlling the transport across the membrane. The most abundant proteins on the lysosomal membrane are the lysosomal associated membrane protein LAMP-1 together with LAMP-2. In addition to these, TRPML1, CLN3 and sialin, for example, are all located on the lysosomal membrane and play a role in lysosomal function. (Ruivo *et al,* 2009) Pathological states manifesting from a misfolded membrane protein prove the important role of these proteins. For example, Niemann-Pick disease type C has been linked with abnormally glycosylated LAMP-1 (Cawley *et al,* 2020), whereas LAMP-2 deficiency causes Danon disease (Nishino *et al,* 2000). Lastly, mucolipidosis type IV is caused by a mutation in the gene coding for TRPML1 cation channel on lysosomal membrane (Sun *et al,* 2000).

The function of lysosomal membrane proteins varies greatly. For instance, LAMPproteins have been shown to play a role in autophagic machinery, cholesterol trafficking, transportation of cytosolic peptides for degradation and lysosomal biogenesis. (Eskelinen *et al,* 2004; Demirel *et al,* 2012) TRPML1, on the other hand, plays a part in Ca2+ release from the lysosomes when autophagic machinery is activated. This machinery is discussed in the next chapter from lysosomes' point of view. The Ca^{2+} release from the lysosomes marks the start of the autophagic process, which in turn activates downstream proteins responsible for upregulation of autophagy-related genes. (Medina *et al,* 2015)

2.1.2 Lysosomes' role in autophagy

Autophagy is a well-preserved catabolic process where biomolecules are transported into lysosomes and degraded into building blocks to be used again in the cell. Autophagic pathway is parallel to the lysosomal maturation pathway, where intracellular material is transferred to lysosomes through autophagy. Autophagy is a vital process in, for example, adaptation to nutrient deprivation during starvation, anti-aging, preventing neurodegeneration, regulating immune response and tumor suppression. (Settembre and Ballabio, 2011) Not only is the lysosomal function impaired in lysosomal storage diseases, but also autophagic machinery is damaged (Spampanato *et al,* 2013).

Autophagy can be divided into three different types: microautophagy, chaperone-mediated autophagy and macroautophagy. Microautophagy refers to a process where lysosomal membrane invaginates transferring cytosol into the lysosome, whereas chaperone-mediated autophagy means transmembrane trafficking of cytosolic proteins into the lysosomes. (Mizushima *et al,* 2010) Macroautophagy is the most studied form of autophagy and the focus of this chapter. Hence, hereafter, macroautophagy will be referred to as autophagy.

When autophagy is stimulated by, for example starvation as discussed before, activated dephosphorylated TFEB relocates from the cytosol into the nucleus inducing DNA transcription of multiple genes. TFEB activation requires upstream activation of calcineurin, which responds to Ca2+ efflux from lysosomes via TRPML1 (Medina *et al,* 2015). Translocation of TFEB to nucleus causes a chain reaction culminating in the formation of double-membrane vesicles within the cytoplasm. These autophagosomes fuse with lysosomes creating an autolysosome. (Ravikumar *et al*, 2010; Settembre *et al*, 2013)

In addition to numerous proteins, this fusion also requires lysosomal acidification. For example, inhibition of V-ATPase by bafilomycin, has been shown to inhibit the fusion of autophagosomes and lysosomes (Yamamoto *et al*, 1998). This inhibition route can be used in *in vitro* research of autophagy. On the contrary, upregulating autophagy can be accomplished through starvation or, for example, with rapamycin treatment, which inhibits mTOR and releases TFEB to relocate to the nucleus. (Ravikumar *et al,* 2004) Impaired autophagy, with a defect in either autophagosome creation or the fusion with lysosomes, in addition to impaired lysosomal function, might cause the symptoms of lysosomal storage diseases discussed later.

In conclusion, autophagy is a crucial process rapidly responding to intracellular stress arising from e.g. starvation and being orchestrated by the vast TFEB-regulated network. This response depends on the acidic lumen of lysosomes that is utilized in the fusion with autophagosomes and is crucial for the catabolizing hydrolases to work. Not only do lysosomes exploit acidic environment and hydrolases for degradation, but they can also discard metabolic byproducts and other cellular waste by exocytosis. Exocytosis is a process which allows the cell to secrete the cellular waste possibly too complex to metabolize. The two-step process culminates in a fusion between lysosome and plasma membrane, after which the contents of lysosome are discarded in the extracellular space.

2.1.3 Lysosomal exocytosis

Lysosomal exocytosis is a crucial cellular secretory pathway including Ca^{2+} independent and –dependent steps is a process of two sequential steps. In addition to secretion, this mechanism is crucial in repairing the plasma membrane of the cells. The same membrane-budding stages are also used intracellularly in the fusion of membrane-coated vesicles with each other, such as when lysosomes and endosomes fuse together. In normal, non-diseased conditions, for most cells, lysosomal exocytosis is only a minor exocytotic pathway, which is mainly used when cells are under stress. This was demonstrated in a study by Rodríguez *et al* conducted in 1997, where the group demonstrated an increase in lysosomal exocytosis in response to an increase in intracellular [Ca^{2+}]. This increase in calcium concentration is a signal of cellular stress, to which TFEB dephosphorylation and thus activation responds to, climaxing in autophagy upregulation. As stated before, this exocytotic pathway can be divided into two sequential steps distinguished by their Ca^{2+} dependency.

In the first, Ca^{2+} independent step, the lysosomes move to close proximity of the cell membrane with the help of Rab proteins that direct the vesicle towards its destination, and motor proteins that move the vesicles along microtubules or actin filaments of the cell cytoskeleton. There are over 60 known Rab proteins, which are all monomeric GTPases, and they work together with Rab effectors. (Alberts *et al,* 2015) The transport-location specific Rab proteins regulate the transportation of the vacuoles into the right place, including the cellular membrane, where the fusion and exocytosis occur. There are multiple different Rab proteins and effectors depending on the cell type. For example in melanocytes, the Rab27a associates with melanophilin and myosin Va and together this tri-protein complex is responsible of the transport of granules from microtubules to actin. (Bossi *et al*, 2005)

The second step in the exocytosis is dependent of Ca^{2+} and involves fusion between the cellular membrane and lysosomes in order to empty the contents of lysosome outside the cell. Increase in the intracellular level of Ca^{2+} induces

lysosomal exocytosis, which follows employment of N-ethylmaleimide-sensitive factor-attachment protein receptors (SNAREs) needed for lipid membrane fusions (Jaiswal *et al*, 2002). SNARE-complex and its regulators attach the lysosomes to the intracellular plasma membrane, after which localized increase in Ca^{2+} concentration induces exocytosis. (Rodríguez *et al*, 1997)

Lysosomal exocytosis is heavily controlled by different pathways within the cell. The before mentioned master controller of lysosomal function, TFEB, has been shown to affect multiple cellular processes involving lysosomes. For example, overexpression of TFEB increased both lysosome biogenesis and Ca^{2+} dependent exocytosis. (Saridello *et al,* 2009; Medina *et al,* 2011) Increase in exocytosis is explained by the regulatory role of TFEB: its downstream target, a cation channel on lysosomal membrane called TRPML1, releases calcium to trigger lysosomal exocytosis. When TFEB is overexpressed in cells depleted of TRPML1, intracellular Ca^{2+} concentration is not increased. (Medina *et al*, 2011)

In addition to these abovementioned regulators of lysosomal function and the role of calcium, the subcellular localization of the lysosomes also affects the result of their activation. Exocytosis rate increases in those lysosomes proximal to the cellular membrane when Ca^{2+} concentration increases (Jaiswal *et al,* 2002). In addition to exocytosis regulation, it has also been demonstrated that increased Ca^{2+} concentration regulates autophagy, and various speculations of the mechanism have been published (Grotemeier *et al,* 2010; Bootman *et al,* 2018). Thus, this network with players such as intracellular calcium, the master regulator TFEB, and its downstream target genes is truly a maze that can only be briefly mentioned in this review.

If exocytosis is to be studied, it can be observed by the expression of LAMP-1 on the cell membrane following the lysosomal fusion with the plasma membrane, since LAMP-1 is only expressed on the lipid membrane of LEs and lysosomes and is exposed for the antibodies by the cellular plasma membrane. LAMP-1 together with LAMP-2 is the most abundantly expressed protein on the lysosomal membrane. (Saftig and Klumperman, 2009) Another protein that

can be detected in exocytosis is TRPML1, the cation channel increasing lysosomal Ca^{2+} efflux to trigger membrane fusion.

Thus, exocytosis could be detected by the presence of LAMP-1 on the cellular plasma membrane after the fusion needed for exocytosis. This was evident on the cellular model overexpressing TFEB in the study conducted by Medina *et al* in 2011. Together with the LAMP-1 detection on cellular membrane, also several lysosome-specific enzymes can be detected from the cell culture medium and thus verify the rate of exocytosis.

As a conclusion, TFEB has a crucial role in regulating both overall lysosomal function and autophagy, the cellular process used to dispose intracellular waste. Lysosomal degradation being the main waste disposal method for endocytosed molecular debris, autophagy is used for intracellular waste, such as misfolded proteins and worn-out cellular organelles. In case of bigger, non-digestible molecules, the cells use exocytosis to dispose intracellular waste.

Hypothetically, these processes could be utilized in repairing the cellular impairments caused by substance accumulation by enhancing the exocytosis or autophagy. These substance accumulation pathologies could be LSDs, but also CNS-affecting accumulation diseases such as Parkinson's disease. Currently, no treatment exploiting lysosomal degradation and autophagy through modulating TFEB activation is in use in the clinics, although recently published studies suggest that these are under investigation. TFEB activation has been proposed to be of use in *in vitro* and *in vivo* parkinsonian neurotoxicity (Wang *et al,* 2020; Zhuang *et al,* 2020), in alleviating diabetic nephropathy both *in vitro* and *in vivo* (Yuan *et al,* 2020), and in treatment of Pompe disease (Spampanato *et al,* 2013). Pompe disease is one of the LSDs where glycogen accumulates due to inefficient acid alpha-glucosidase causing a severe myopathy (Spampanato *et al,* 2013). These storage diseases share common pathological processes discussed in the next chapter.

2.2 Lysosomal storage diseases

First defined by Hers in 1963, lysosomal dysfunction causes macromolecules to accumulate progressively in cells, and this type of pathogenic conditions are classified as lysosomal storage diseases (LSDs) (Lieberman *et al,* 2012). LSDs are distinguished by an excessive buildup of metabolic byproducts, which negatively affects the homeostasis of lysosomes causing rupture of the acidic organelles into cytoplasm triggering cell death. This leads to dysfunction of different tissues and organs, which results in an often untreatable pathological state. (Boya and Kroemer, 2008; Parkinson-Lawrence *et al,* 2010) Accumulation of undigested metabolic byproducts causes the lysosomes to enlarge, which is a histological characteristic of LSD cells. There are over 70 different LSDs collectively affecting approximately 1:7700 live births (Meikle *et al*, 1999). These diseases are orphan diseases caused by a mutation in a gene coding for an enzyme affecting lysosomal function (Samie and Xu, 2014). The mutated enzymes can be lysosomal hydrolases directly affecting lysosomal degradation of lipids, or proteins indirectly affecting lysosomal substrate degradation (Parkinson-Lawrence *et al,* 2010; Schulze and Sandhoff, 2010).

LSDs are progressive diseases affecting multiple organs, especially tissues with significant amount of postmitotic cells. The usual symptoms, such as mental retardation, neurodegeneration and motoric disabilities manifest through the affected organs, including brain, liver, spleen, eye and muscle. LSDs often result in premature death after a decline in both physical and mental health usually arising from early childhood. (Samie and Xu, 2014; Platt, 2018) Several therapeutic approaches have been developed for LSDs, which vary according to the specific disease pathology. Therapy options can be divided into two categories based on the target: disease specific therapies and therapies targeting downstream targets of the pathogenic cascade. Treatment options, regardless of the category, include bone marrow transplantation (BMT), ERT, gene therapy, small molecule chaperons and substrate reduction therapy (SRT). In BMT, the patient receives a bone marrow transplant from a healthy donor, after which enzymatically capable blood cells, e.g. macrophages, replace the patient's own macrophages and contribute to

clearance of accumulated product. In addition, healthy cells obtained from the donor can repair enzyme function in cells through cross correction. This means enzyme exocytosis through the before mentioned extracellular detour and endocytosis of the circulating enzyme through MPRs. ERT exploits the same pathway, but in ERT, the working enzyme is given exogenously. (Macauley, 2016) Gene therapy, on the other hand, aims to recover the enzyme function intrinsically by targeting the mutated gene with a viral vector delivering the correct sequence and thus repairing the mutation. (Sands and Davidson. 2006) Chaperons are small molecules that bind to the readily translated protein chain and stabilize the correct folding structure, whereas substrate reduction therapy aims at the reduction of the substrate amount by small molecules that inhibit the synthesis rate of the accumulating substrate. (Macauley, 2016; Banning *et al,* 2016) Several different approaches have been developed and studied for LSD treatment. Available therapy options depend on the disease and range from several different options in Gaucher disease to no treatment options in aspartylglucosaminuria (AGU).

Gaucher disease, an LSD caused by an impaired acid-β-glucosidase function has the most approved treatment options available. There are five different U.S. Food and Drug Administration (FDA)-approved treatment options, of which the European Medicines Agency (EMA) approves four. The four EMA-approved treatment options are imiglucerase (ERT), velaglucerase (ERT), miglustat (SRT) and eliglustat (SRT). In addition to Gaucher disease, several other LSDs' have ERTs available, for example agalsidase-α for Fabry and alglucosidas alfa for Pompe disease. (Beck, 2017) Several other treatments have been granted the orphan drug designation status and will probably provide ease in the disease symptoms in several lysosomal storage diseases. Despite several treatments being granted marketing authorization, there is no curative treatment for any LSD available. Thus, the unmet medical need for both symptom alleviating treatment and curative treatment remains high.

Although different diseases with unique pathology, all LSDs are lysosomal disorders affecting a wide range of tissues both in CNS and periphery. Evidently, the lysosomal function is one of the key mechanisms within the cell

regulating the homeostasis of catabolic and anabolic pathways. In LSDs, both lysosomal function and autophagy are impaired. (Spampanato *et al,* 2013)

2.3 Aspartylglucosaminuria

Aspartylglycosaminuria (AGU) is a lysosomal storage disease where aspartylglucosaminidase (AGA) activity is diminished. The lack of enzyme activity leads to accumulation and increased secretion of glycopeptides, particularly aspartylglucosamine (GlcNAc-Asn). (Dunder *et al*, 2000) Being part of the Finnish disease heritage, most of the disease cases can be found in Finland. The carrier rate is around 1:40, and the autosomal, recessively inherited disease incidence rate is about 1:18 000 (Norio, 2003).

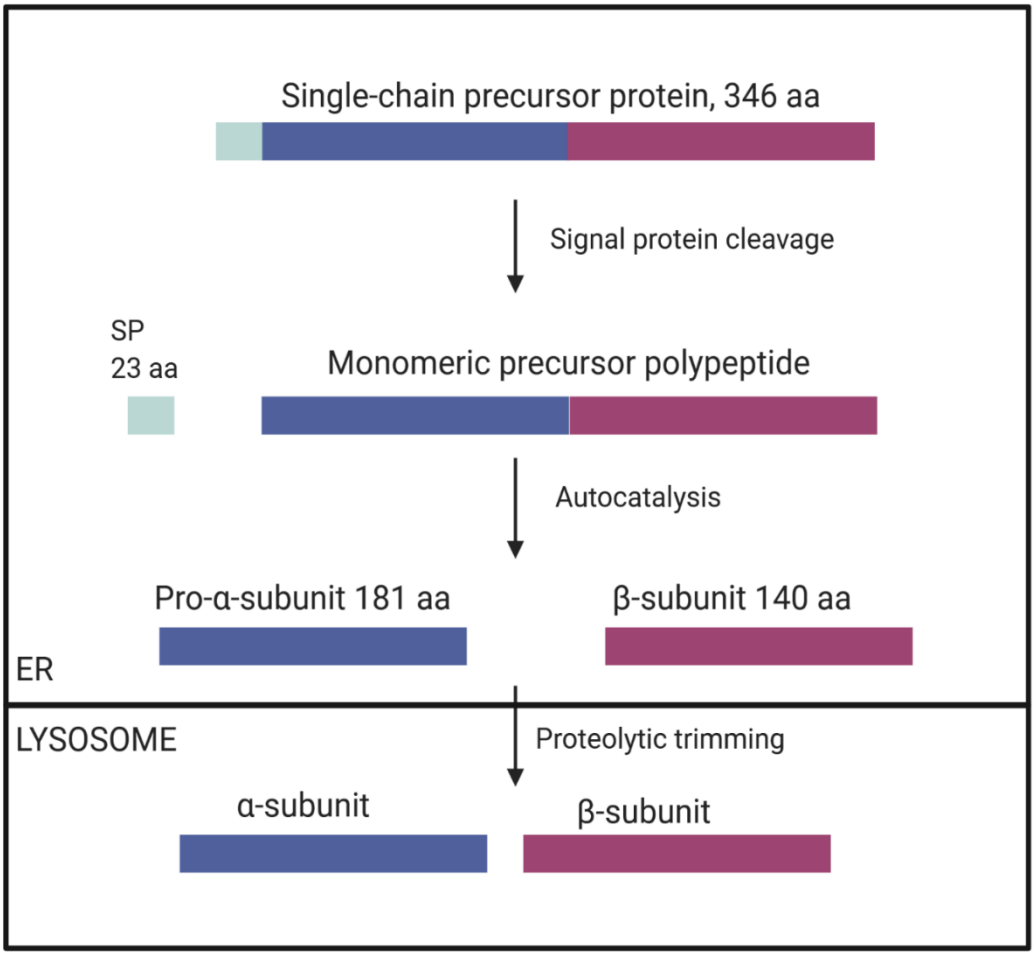

Figure 2. The cleavage of AGA into its subunits and transportation from ER to lysosome. SP=signaling peptide. Adapted from Kelo, 2013.

Under normal conditions, AGA is synthetized in the ER, where it undergoes post-translational changes before autocatalytical cleavage into two subunits, α and β (**Figure 2**). These subunits form a heterotetramer, which is held together by noncovalent forces, constituting the active form of AGA enzyme. (Oinonen *et al,* 1995) The newly formed heterotetramer ($\alpha_2\beta_2$) is transferred to lysosomes after it is tagged with M6P, as discussed in chapter 4.1.1. After transportation to lysosomes, an additional cleavage occurs for the C-terminal ends of both subunits. However, this has no effect on the enzymatic activity but rather precedes an important step: formation of intrasubunit disulfide bridges between eight cysteine residues (McCormack *et al,* 1995; Riikonen *et al*, 1995). Formation of disulfide bonds is crucial for the stabilization of the enzyme and correct tertiary structure, and thus, for the function of AGA (Dunder, 2010).

AGA gene is located in chromosome 4q32-q33, where also the disease-causing mutations are located. There are two mutations identified in Finnish population causing the disease: AGU_{FIN} major and AGU_{FIN} minor. (Norio, 2003) In the AGU_{FIN} major, two point mutations in *AGA* have been found of which one causes the inactivity of glycosylasparagine, and this point mutation is responsible for 98% of the Finnish AGU patient cases. Thus, this founder mutation is termed AGU_{FIN} major mutation. (Dunder, 2010) This major mutation is responsible of two amino acid substitutions, Arg161Gln and Cys163Ser. The latter serine is crucial for the formation of intramolecular disulfide bridges and thus, this substitution results in misfolded protein chain and an inactive enzyme, causing the accumulation of the aspartylglucosamine. The AGU_{FIN} minor is a two base-pair deletion in the second exon of *AGA* causing a frameshift mutation resulting in premature termination of the translation. (Isoniemi *et al*, 1995) In addition to these two major mutations recognized to be in abundance in the Finnish individuals affected with AGU, more than 30 different mutations have been identified around the world. The other mutations affect the protein product in many ways, for example resulting in incorrect folding, incorrect cleavage of the proenzyme into its subunits, too early stop codon, or shift in reading frame. (Ikonen *et al,* 1991) What is common to all

these patients is impaired enzyme function of AGA and accumulation of its substrate. In addition, all the mutations are recessive and thus, from the disease pathology point of view, one copy of the correct gene coding for the enzyme is enough for the pathology to be absent.

2.3.1 Clinical picture

AGU can be diagnosed from urine, detecting the secreted aspartylglucosamine (Mononen *et al,* 1988). In addition, a DNA test can be done to confirm the disease from the mutations in *AGA.* Accumulation of the glycopeptides causes severe mental retardation, coarse facial features and premature aging (Arvio *et al*, 2004). In the childhood, patient has an abnormally slow but positive mental and psychomotor development. In years 15-25, a stable state or slow decline in both mental and physical health is seen, followed by a steep decline after the plateau. Patients rarely live beyond 50 years. One in three patients also suffer from epilepsy, twenty percent have an associated psychiatric disorder and five percent rheumatoid arthritis. (Arvio *et al*, 1993 & 1998)

In recent years, studies on cognitive capabilities and brain structure of AGU patients have been conducted. Cognitive capabilities of AGU children remain significantly lower than in age-matched healthy controls. The AGU children studied, aged 7-14, did not reach the average developmental level of healthy 6-year-old children. In addition, the developmental score did not improve with age, even if previous studies suggest a slow but positive learning curve for AGU children. (Arvio, 1993; Harjunen *et al,* 2020) In a brain MRI study conducted by Tokola *et al* in 2015 cerebellar or cerebral atrophy was found in almost all AGU patients investigated in addition with poor differentiation between grey and white matter, which was seen in all patients imaged. These studies highlight the cognitive impairment coupled with the disease progression in the CNS, which is caused by the neuronal damage thought to result from the accumulation of GlcNAc-Asn.

Although the clinical picture of the disease is somewhat characterized and both genetic and molecular reasons behind the impaired lysosomal function are known, the cause of the symptoms is not clear. Lysosomal dysfunction and accumulation of glycopeptides explain the symptoms and the decrease in mental and physical health, but molecular mechanisms and the causes behind the progressive clinical picture remain unresolved. Because of the unknown aspects of the disease and versatile symptoms, it can be hypothesized that a significant portion of the cases remains underdiagnosed. This could be the case especially in countries where the disease heritage does not include lysosomal storage diseases, contrary to Finland, where the clinical knowledge of LSDs is relatively good based on the homogenous population and the disease heritage including LSDs.

2.3.2 Treatment options available

Currently, there are no medicines available for the treatment of AGU, although bone marrow transplantation (BMT) and a small molecule chaperone therapy have been studied in human patients. In a follow-up study by Arvio *et al* in 2001, seven AGU patients between the ages of 1-10 received a BMT. After a follow-up period of one to seven years, two of the seven patients who were followed for the longest period were more severely mentally retarded than the AGU patient control group. The other five transplantations were successful, but the follow-up period was inadequate to prove effectiveness of the treatment. The research group concluded that BMT is not enough to restore the AGA function in patients with AGU or that the BMT should be done early in infantry.

Recently, a set of small molecules have been studied for use in pharmacological chaperone therapy for AGU. (Banning *et al,* 2016) The group studied different mutations and their response to the molecules in an *in vitro* setting using primary cells obtained from patients. The molecules studied were betaine, glycine and aspartate, which were chosen by their potential to use as pharmacological chaperones in stabilizing the AGA enzyme structure. All three

compounds were found to increase AGA activity within the two disease-causing mutations studied, AGU_{FIN} and Thr122Lys, both of which show inadequate AGA activity. However, when a clinical relevancy study for all three compounds was conducted with purified recombinant AGA, in order to see if the molecules inactivate the enzyme itself in higher concentrations, only betaine proved to not affect the enzyme function itself in bigger concentrations. Thus, out of these three compounds, betaine was chosen to advance to a clinical study for patients with the researched mutations. This clinical study is currently ongoing. In addition, betaine is approved for clinical treatment of homocystinuria by both EMA and FDA under the trade name Cystadane. (European Medicines Agency, Cystadane: EPAR; clinicaltrials.gov: NCT01838941)

In addition to these abovementioned small molecules studied, another molecule progressed to further studies. Amlexanox proved to have potential in an *in vitro* setting in stabilizing the enzyme structure in disease cases resulting from a nonsense mutation. (Banning *et al,* 2018) This molecule was shown to increase AGA mRNA levels in patient fibroblasts with Ser72Pro and Trp168X mutations. Patients with nonsense mutations like this exhibit less severe disease pathology and they have more residual enzyme activity than patients with the AGU_{FIN} mutations and thus, this treatment option cannot be used for the more severe point mutations.

From a drug developmental perspective, a translational disease model must be available. For AGU, two different types of mice models have been developed, both of which are knockout models (Kaartinen *et al,* 1996; Jalanko *et al*, 1998; Tenhunen *et al,* 1998). The first type has the entire *AGA* gene knocked out ($Aga^{(-/-)}$), (Kaartinen *et al,* 1996; Jalanko *et al*, 1998) whereas the second model type mimics the AGU_{FIN} major mutation and thus only short sections of the gene are knocked out (Tenhunen *et al,* 1998). It must be kept in mind that to be properly translational, a patient mutation is always a closer representation of the real disease compared with a total knock-out model. This might, however, mean that symptoms do not manifest in mice as they are represented in the human patients, which presents challenges to the *in vivo* research of the disease and the translatability of the model. Luckily, this is not

the case with either of the AGU mice models. The *in vivo* models for AGU are highly translational, exhibiting same clinical manifestations and progressive nature of the symptoms similarly to the progression seen in patients. Histologically, the $Aga^{-/-}$ mice show enlarged lysosomes in both CNS and peripheral tissues, which resembles the findings in patient tissues. (Kaartinen *et al*, 1998) In addition to the histological findings, the $Aga^{-/-}$ mice show significantly affected gait, e.g. dragging of their hind legs. It has also been reported that the mice have deprived coordination and balance correlating with the motor function impairment of AGU patients and the mice only live about half as long as the healthy mice. (Gonzalez-Gomez *et al,* 1998)

Thus, both *in vitro* and *in vivo* models have been established for AGU, but no breakthrough for therapy applications has been developed. According to Mononen *et al* (1995) and Dunder *et al* (2000), when AGA is introduced *in vitro* to a cell culture from AGU patient, the enzyme is endocytosed and function of aspartylglucosamine is restored. However, in an *in vivo* model, the enzyme replacement therapy restores the enzyme function in other tissues but not the brain, where GlcNAc-Asn accumulation causes the most serious developmental defects. The difficulties for the enzyme to cross into the brain is due to the protective nature of BBB, which inhibits the access of AGA to the CNS. Regardless of both *in vitro* and *in vivo* models and studies of AGU, no treatment benefiting the patients has been developed.

2.4 Summary

Clearly, there is a vast unmet medical need in terms of treatment options for lysosomal storage diseases. This applies to all LSDs, including AGU, one of the severe Finnish heritage diseases and the focus of this study. Since the disease is rare, about 1:18 000 live births affected in Finland, and no cure is available, it can be hypothesized that the disease is also underdiagnosed at least on global scale. AGU is diagnosed from urine in terms of secreted GlcNAc-Asn, and if a treatment was available, diagnosing yet asymptomatic newborns would be reasonable and would possibly increase the disease prevalence. In addition to the clear unmet medical need, the underlying

pathological mechanisms causing the symptoms and the progressive nature of the disease are not fully understood, and a lot remains to be discovered. Patients affected show decline both physically and mentally, and what causes this progressive nature of the symptoms in both periphery and CNS remains to be discovered. The accumulation of a metabolic product due to malfunctioning enzyme is the primary disease-causing process, but the molecular mechanisms following lysosomal accumulation are not completely known.

In order to be able to treat patients suffering from lysosomal storage diseases, the disease pathology needs to be understood and the differences between healthy and pathological conditions characterized. Characterization of the differences is the key concept in this thesis and aim of the research. By utilizing various biomedical research methods, the aim was to unravel the cellular and molecular differences within the cells underlying the pathological state and the symptoms manifesting in the AGU patients. The research focused on the enzymatic differences within AGU and healthy cells and on establishing a reliable model for lysosomal storage diseases. This work enables the future research in Orion focusing on methods aiming to restore the enzymatic function or reducing the accumulation of substrates with other means within the selected LSDs.

3. Results

3.1 Cell maintenance

Both lymphocytes and fibroblasts from healthy and AGU-patient donors were maintained throughout the study. Lymphocyte growth media supported the growth of lymphocytes and no differences in growth pattern were observed between the healthy and AGU patient cell lines. Lymphocyte cell cultures were passaged as the supplier instructed.

Fibroblasts exhibited distinct differences both morphologically and in their growth patterns. The growth was poor with especially the AGU fibroblasts, and thus, the growth media for AGU fibroblasts was supplemented with 20% fetal bovine serum to facilitate the growth. Despite the modifications, growth rate of the AGU vs healthy fibroblasts continued to differ along the passages. The healthy control fibroblasts exhibited a steady growth curve with also larger passages, but around passage 20, the growth rate of AGU fibroblasts started to decline. Morphologically, the AGU fibroblasts did not form a uniform, systematically growing cell layer as did the healthy control fibroblasts. (**Figure 3**) AGU fibroblast vessels contained significantly more cell debris floating in the medium and the cells had debris attached to the cell surface as well. Individual AGU cells were not morphologically comparable with the healthy fibroblasts. Some of the cells showed a round phenotype with a tumor-like appearance, which was not seen in the healthy cell culture. Cell culture cross-contamination with a cancerous cell line, however, is not possible.

When passaging the cells, the healthy controls attached to the bottom of the growth vessel significantly better than the AGU cells and thus, there was less cell death occurring within the control flasks than with the AGU fibroblasts.

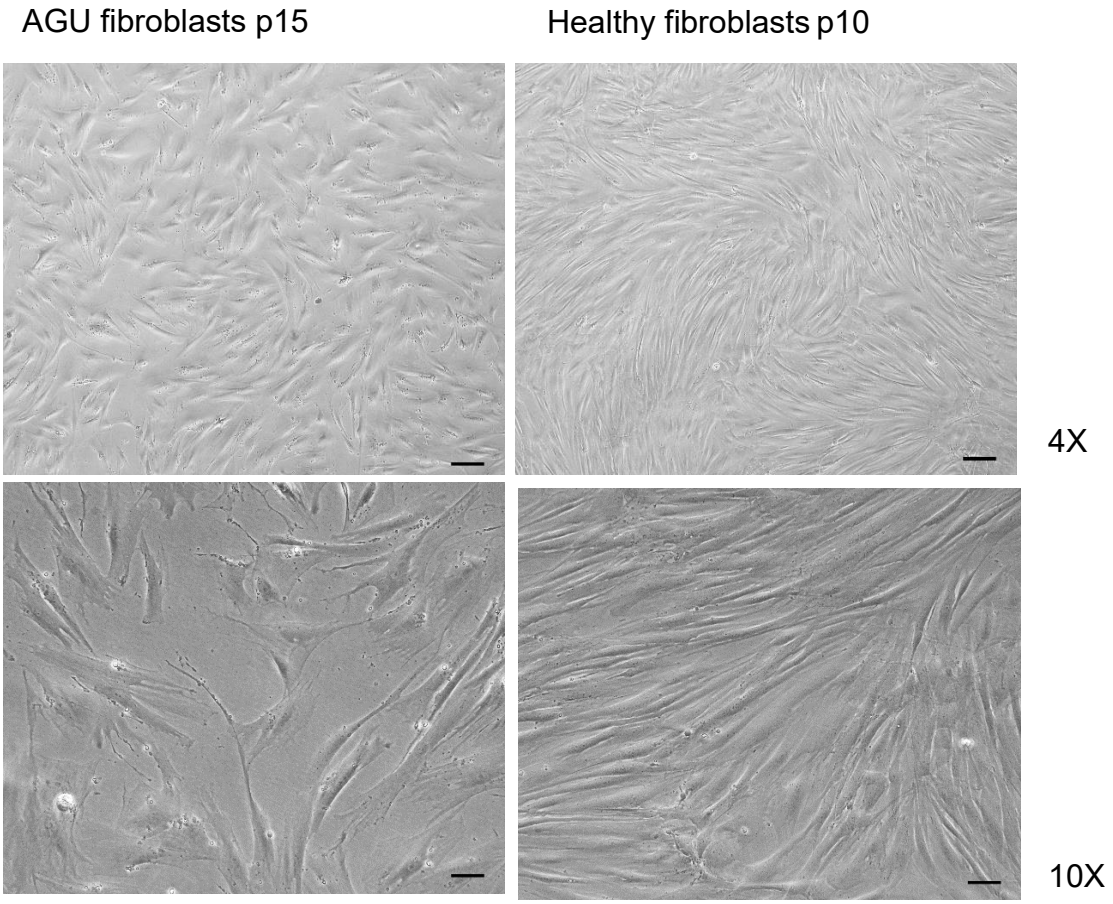

Figure 3. Microscopic images of both AGU and healthy fibroblasts. 7 days after last passage to same confluence with 4X and 10X magnifications. AGU fibroblasts present a less organized cell layer and a slower growth rate when compared to the healthy fibroblasts, which grow in an organized cell layer. Scale bar 100 µm in 10X and 250 µm in 4X images.

Detaching fibroblasts was optimized with 0.04%, 0.08%, 0.16% and 0.25% trypsin in 0.53 mM EDTA in HBSS, and 0.25% trypsin in DPBS. The cells detached adequately with only the highest trypsin concentration. Approximately five passages were grown parallel to investigate the possible morphological changes caused by the higher trypsin concentration, but no changes were observed and thus the detaching protocol was modified to use one DPBS wash followed by 0.25% trypsin in DPBS until the cells detach to ensure throughout detachment and proper subculture progenitors.

3.2 Enzyme activity measurements

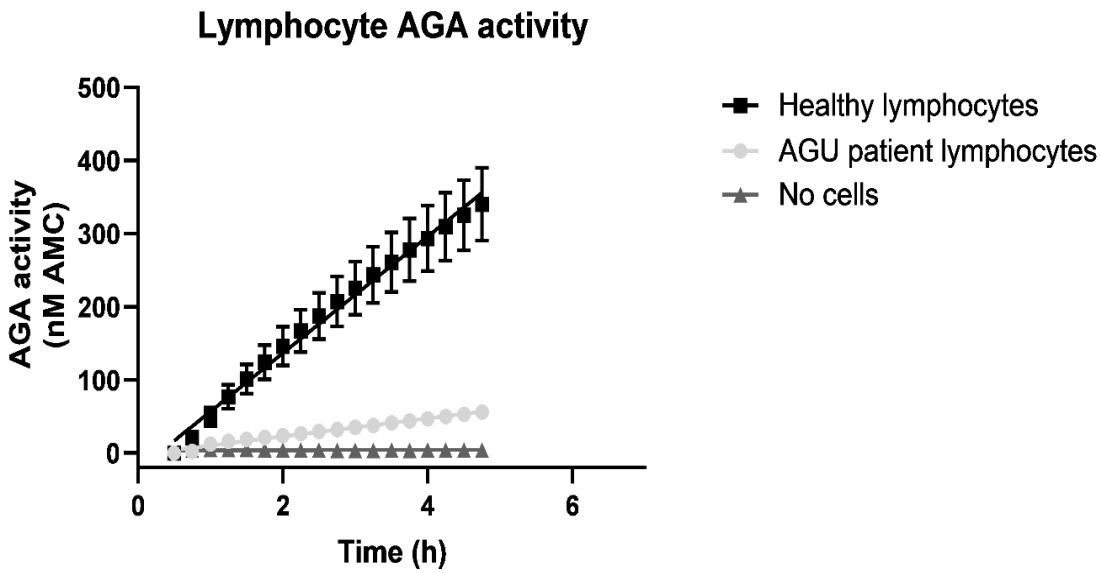

Figure 4. The enzyme activity of AGA measured every 2 minutes for 6 hours. The activity in healthy cells is stable and about 8-fold compared with AGU lymphocytes. Mean + SD of each time point shown.

Enzyme activity was measured with a fluorescent ligand, Asp-AMC, emitting a signal when cleaved by the AGA enzyme to free asparagine and fluorescent AMC group. The activity of AGA was stabile in both healthy and patient cell lysates throughout the reaction. Healthy cells exhibit an activity sufficient to break down the metabolic product causing AGU, but in AGU cells, the enzyme activity is not enough to metabolize GlcNAc-Asn. Although the enzyme activity in AGU cells is not completely absent when comparing with a control sample without any cell lysate, it is approximately one tenth of the activity in the healthy samples and thus only emits a fracture of the signal that of healthy cell lysates. This can clearly be seen in the 6-hour measurement, where the signal emitted from the fluorescent substrate cleavage is constant (**Figure 4**).

The enzyme activity was also measured with 24-hour end-point measurement. This measurement confirmed that the signal is steady even for longer periods of time, which suggests that this study setting is suitable for modeling the biological state of the cell lines and their differences. In **figure 5**, a graph from

the end-point measurement shows a significantly higher ($p < 0.0001$) enzyme activity in healthy cells compared with the AGU cells.

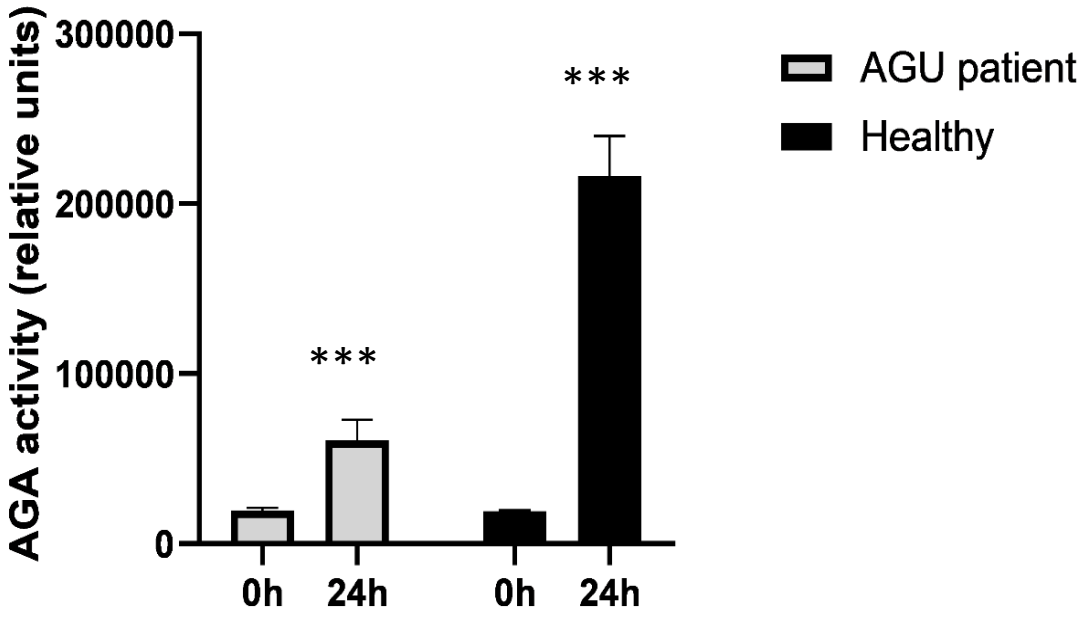

Figure 5. Aga activity measurement at 0 h and 24 h from both AGU and healthy cell lysate. AGA activity can be seen in both, but in healthy cells AGA activity is significantly higher ($p < 0.0001$) after 24 h compared with the AGU cells, in which the activity is five-fold smaller.

The Km value for AGA enzyme within the healthy lymphocyte lysate was determined from a standard curve with Michaelis-Menten equation (**Figure 6**). The Km value for the healthy lymphocyte AGA enzyme was determined to be 17.01. This indicates that the concentration at which half of the enzyme is bound with substrate is 17.01 µM. Previously, Km for wild type AGA has been reported to be 93 µM (Mononen *et al,* 1993), 2500 µM (Tikkanen *et al*, 1996) and 444 µM (Saarela *et al*, 2004) depending on the protocol used.

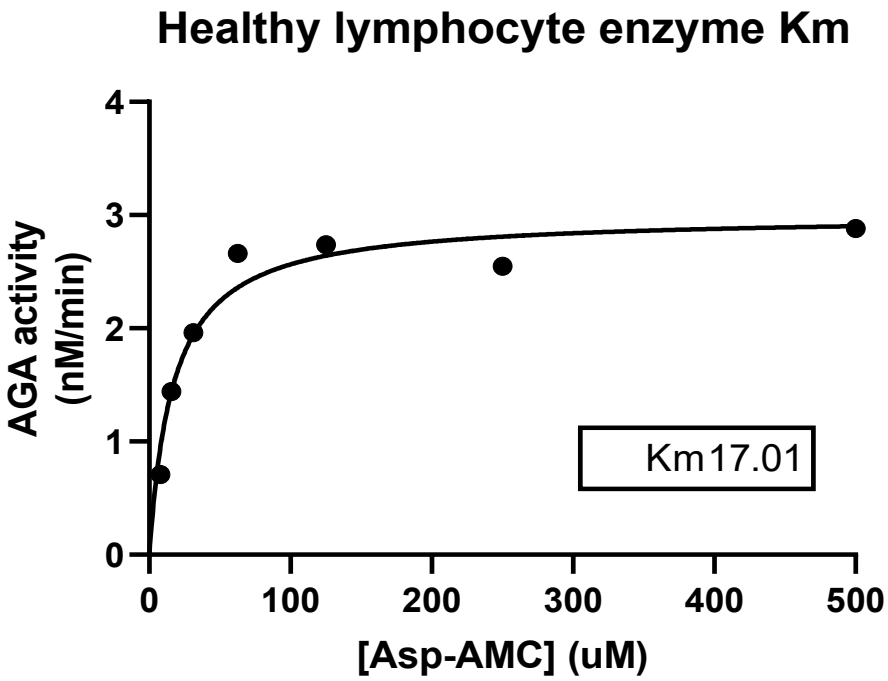

Figure 6. Km value of AGA in healthy lymphocytes. Calculated with the Michaelis-Menten equation.

3.3 GlcNAc-Asn measurement

The amount of AGA substrate within the cell was measured with mass spectrometry analysis. The analyses were done from the GlcNAc-Asn amounts from lymphocyte lysates prepared from healthy and AGU cells. In **figure 7**, the mass spectrometry results show a significantly higher concentration ($p<0.0001$), approximately 20-fold, of GlcNAc-Asn in the AGU lymphocytes compared with the healthy cell lysate.

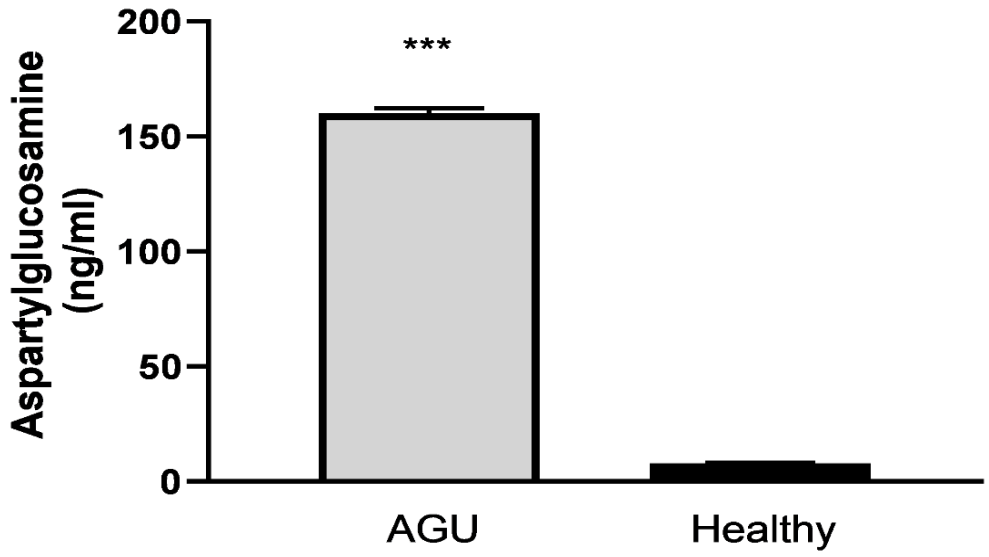

Figure 7. Aspartylglucosamine concentration in AGU and healthy lymphocytes. The concentration in AGU lymphocytes is significantly bigger ($p<0.0001$) than in healthy lymphocytes, in which functioning AGA enzyme cleaves GlcNAc-Asn inhibiting the lysosomal accumulation. Mean + SD shown.

Recombinant enzyme restores the enzyme activity and thus decreases the amount of the enzyme substrate accumulated within the cells. This can be seen from the **figure 8** showing the amount of the substrate, GlcNAc-Asn, within AGA treated AGU and healthy control cells, and untreated AGU cells. The cells were grown for four days under normal culturing conditions, and in addition, 1 µg/ml of recombinant AGA was added to the medium in one flask of the AGU cells, approximately 200 000 cells/ml. After four days, the cells were lysed and the amount of the substrate in the cells was measured with mass spectrometry analysis. The AGU cells grown with aspartylglucosaminidase had a significantly decreased ($p=0.0002$) amount of GlcNAc-Asn compared with the untreated cell line and thus, had an increased enzyme activity. As seen from the **figure 8,** the level of GlcNAc-Asn is only slightly larger in (3-fold) AGA supplied AGU lymphocytes than the amount of the substrate in healthy cells, compared with the 20-fold difference between healthy and untreated AGU cells. This suggests that the active enzyme is able to cross the cell membrane and enter the lysosomes, and that the enzyme

activity is preserved for at least four days in culturing conditions that mimic the physiological state.

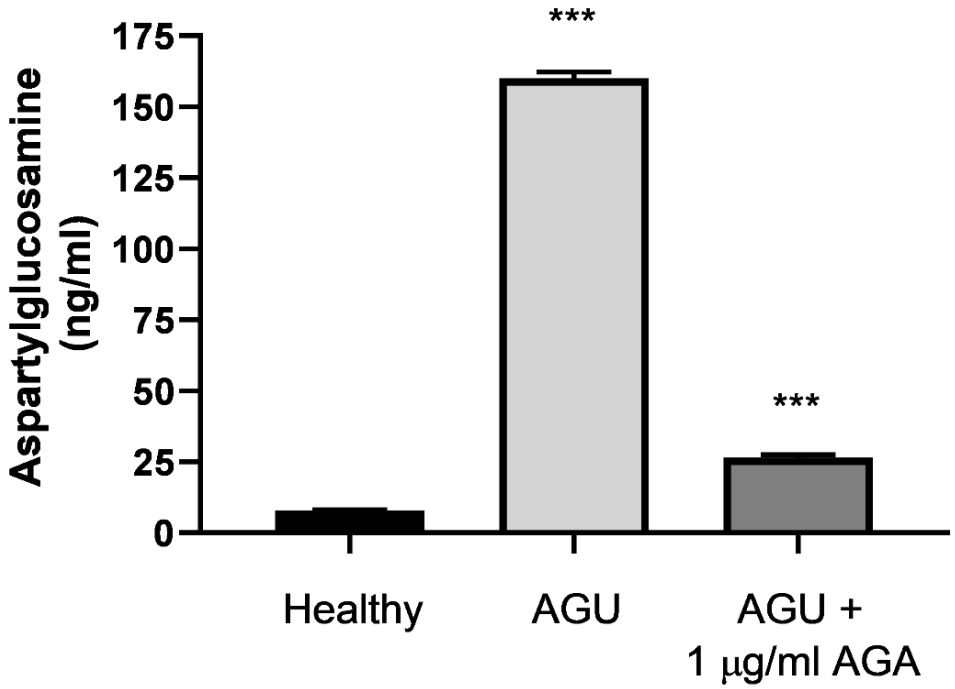

Figure 8. GlcNAc-Asn amount in healthy, AGU and AGU treated with recombinant AGA lymphocyte lysates. Substrate amount decreased significantly (p=0.0002), about six-fold, when recombinant AGA was added to cell culture medium. Mean + SD shown.

3.4 Immunostaining

3.4.1 LysoTracker DeepRed timepoint study

LysoTracker timepoint imaging with live cells was conducted for 18 hours, with one image every 20 minutes. From this timepoint measurement study (**Figure 9**), LysoTracker staining and starvation time were further optimized, and the optimal imaging timepoint was defined to be up to eight hours, after which the differences begin to fade. From these results the differences between the AGU cells and healthy controls were evident. AGU cells had significantly higher spot intensity in analysis compared with the healthy cells, where signal was relatively small throughout the experiment. This suggests, that the AGU fibroblasts under normal conditions had either bigger lysosomes due to the accumulated GlcNAc-Asn or bigger number of lysosomes giving a higher relative signal per well compared with the healthy fibroblasts.

Comparing the signal curves on **figure 9** it can be seen that starvation of the healthy cells increased the LysoTracker signal to the same level as the AGU cells in normal medium. A significant increase can be seen in both healthy and AGU cells between starved and normal conditions. Starved AGU signal is clearly higher than the other signals, and healthy control cells without starvation emit the lowest signal. The signals remain relatively stable up until approximately time point 8 h, after which the signal starts to decrease in cells with highest signal and increase in cells with the lowest signal thus making the relative differences smaller. Thus, starvation increased LysoTracker signal in both cell types. This would imply that the number of lysosomes increases in response to nutrient deprivation and lysosome biogenesis machinery is activated, and this response seems to function adequately in both cell lines. In conclusion, the AGU cells seem not to be impaired in their ability to employ the lysosomal biogenesis process and that the baseline of lysosomal signal is elevated even under non-starved conditions in AGU cells compared with the healthy cells.

3.4.2 Co-location of LAMP-1 and LysoTracker Deep Red

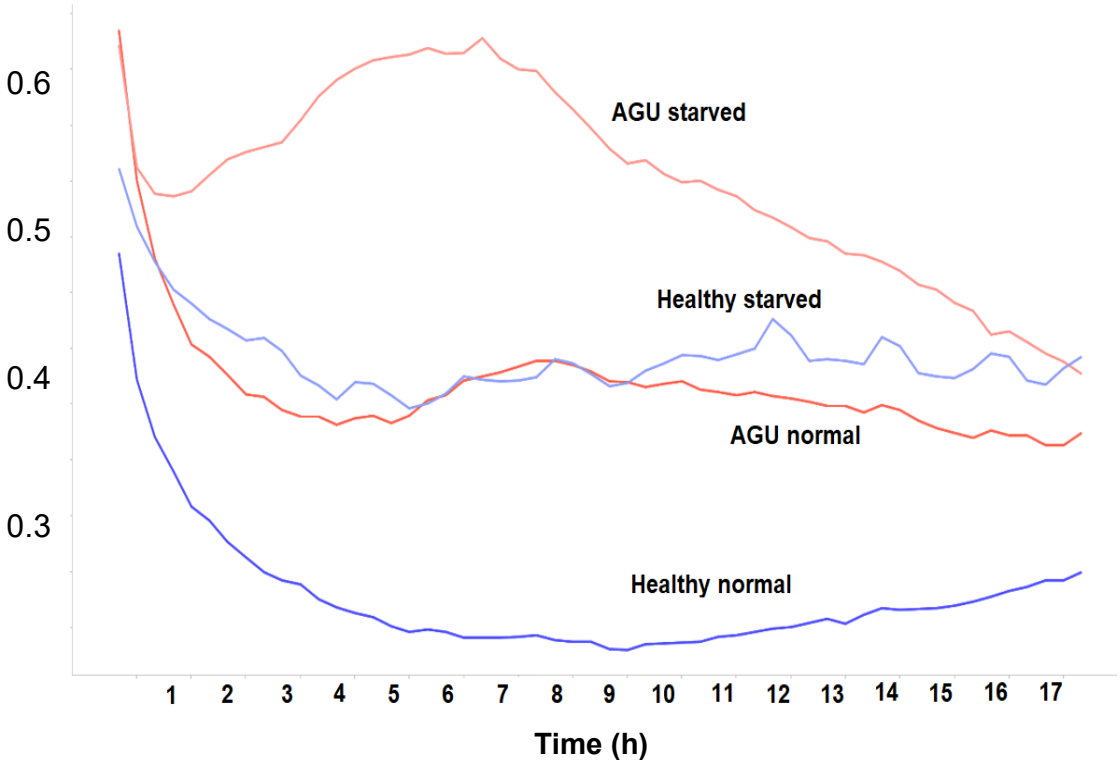

Figure 9. Time point measurement of LysoTracker signal with AGU and healthy fibroblasts under starved and normal conditions. According to the results, the optimal time point for imaging starvation response with LysoTracker is at around 6 h after the start of starvation. The y-axis represents relative units.

To compare the LAMP-1 antibody and LysoTracker on their efficiency to recognize lysosomes, a co-location study was conducted. Fibroblasts were incubated with LysoTracker Deep Red before fixation and stained with antiLAMP1 to study the colocalization of LAMP1 antibody and lysosomes. LAMP-1 signal overlapped with 20-30% of the LysoTracker signal, whereas LysoTracker signal overlapped with over 50% of the LAMP-1 signal (**Figure 10**). Thus, the anti-LAMP-1 antibody is not specific enough to be used in further studies concentrating on intracellular compartmentalization of lysosomes and LysoTracker is to be used in future experiments to obtain as reliable results as possible.

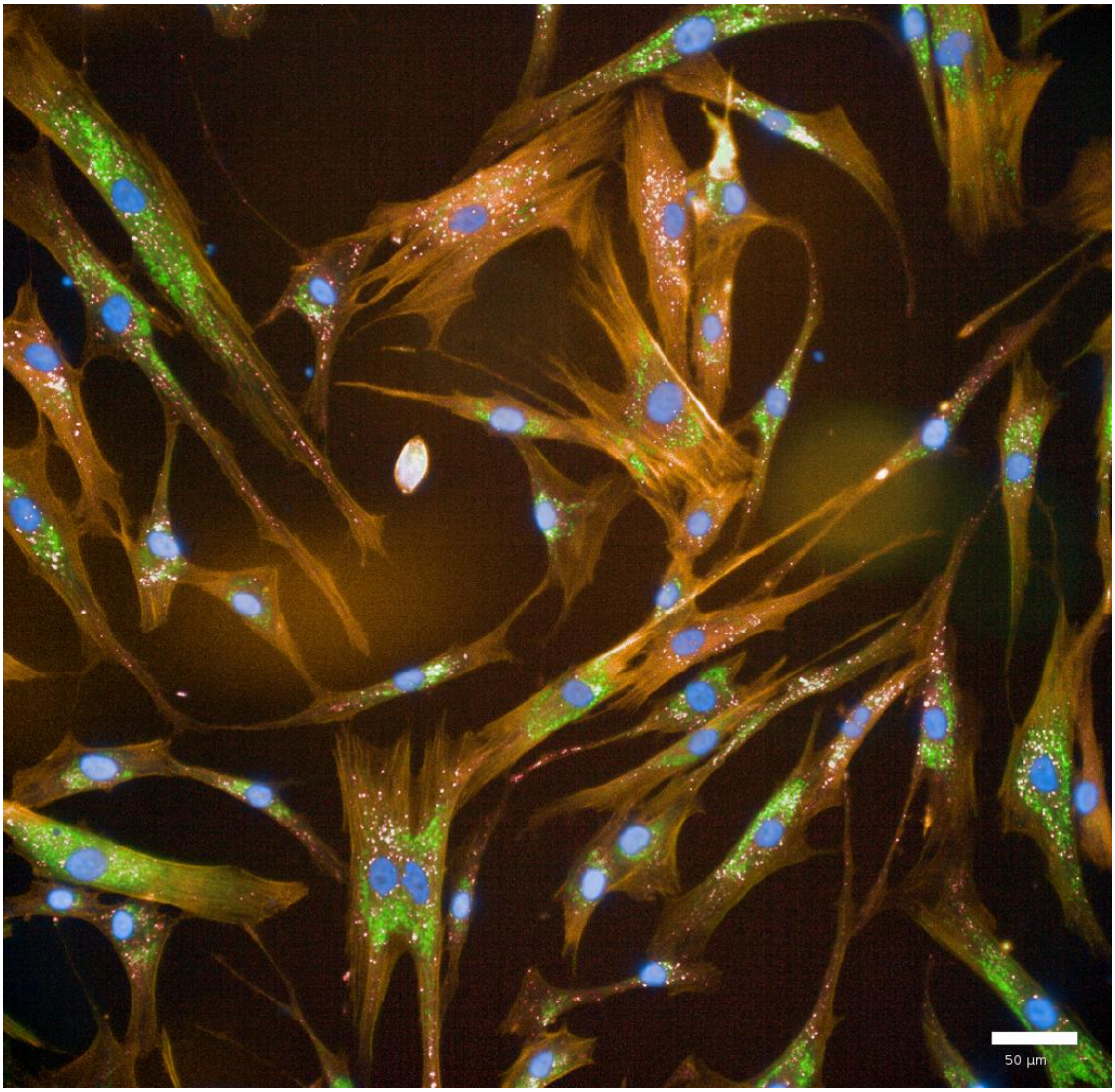

Figure 10. Co-localization study of LAMP-1 and LysoTracker. LAMP-1 in green and LysoTracker in red. LysoTracker stains lysosomes more specifically, 50% of LysoTracker overlaps with LAMP-1 staining. LAMP-1 staining has more unspecific staining, which looks blurry. 20-30% of LAMP-1 staining overlaps with LysoTracker. 50 µm scale bar, orange staining=phalloidin, blue staining=DAPI.

3.4.3 Starvation

Starvation experiments were conducted with plated fibroblasts from both healthy and AGU individuals. Starvation was induced by depleting the growth medium from FBS. Based on the time point study with LysoTracker DeepRed,

starvation was decided to be studied for 6 h. For the last 30 minutes of the starvation, LysoTracker DeepRed was added to the wells. After starvation, the cells were washed, fixed, stained with phalloidin and DAPI and imaged. The images were analyzed for the localization of the stained lysosomes, by their distance from the nucleus. This was done utilizing the software in the imaging system, which analyzed the LysoTracker DeepRed staining according to the distance from the nucleus. The cells were divided into perinuclear and peripheral areas, which determined the localization of the lysosomes. These results were exported to GraphPad Prism for further statistical analysis.

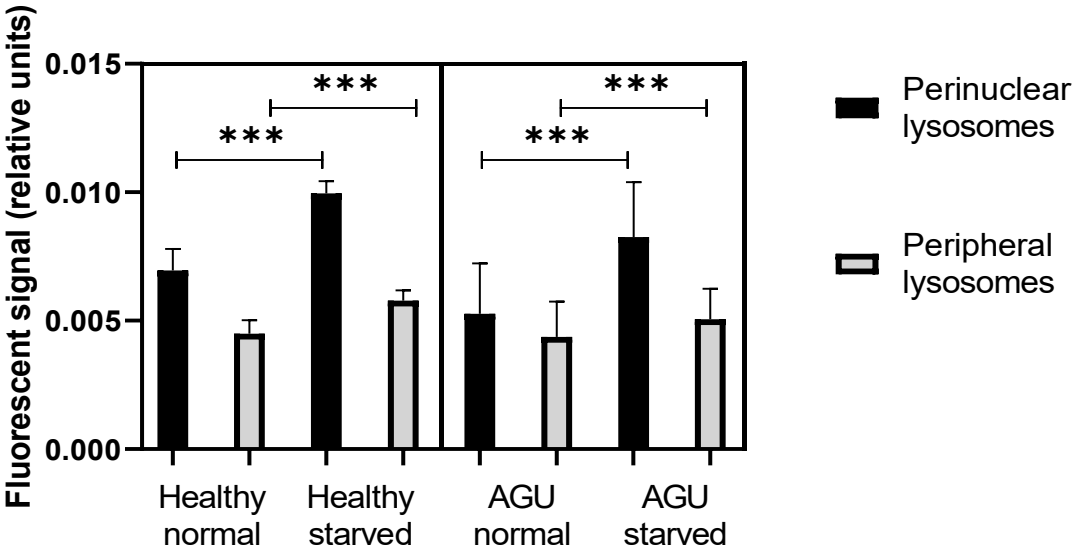

Figure 11. Lysosome positioning in response to 6 h starvation in AGU and healthy fibroblasts. The perinuclear lysosomal signal increases significantly in response to starvation in both cell populations ($p<0.0001$). Perinuclear increase after starvation is more significant in both cell lines when comparing with the non-starved condition. In addition, the peripheral signal in both healthy and AGU ($p=0.0135$ and $p=0.0337$, respectively) cells increased significantly in response to starvation. Mean + SD shown.

By analyzing these photos, the differences between the starved and normal conditions were clearly visible (**Figure 11**). When starved, the cells relocate the lysosomes to perinuclear areas, which is seen from the change in the intensity of the LysoTracker DeepRed signal within perinuclear and peripheral areas in the cells. Comparing the response to starvation between healthy and AGU patient fibroblasts, the lysosome relocation response seems to be similar.

In both cell lines, starvation mobilizes the lysosomes towards the perinuclear area, which leads to an increase in LysoTracker DeepRed signal closer to the nucleus.

In periphery of the cells, the signal is not significantly altered in either of the cell lines, which would imply that the increment of signal perinuclearly is partly due to lysosomal biogenesis. In both cell lines, the perinuclear signal increased statistically significantly in response to starvation ($p<0.0001$ in both healthy and AGU cells). This suggests that lysosomal biogenesis is increased in both cell lines when the cells are deprived of nutrients. In addition, the peripheral signal in both healthy and AGU cells increased statistically significantly under starvation ($p=0.0135$ and $p=0.0337$, respectively). This increase was, however, notably smaller than perinuclear increase.

Another 96-well plate of healthy and AGU fibroblasts was stained similarly to the previous starvation study. The cells were imaged after 6-hour starvation, fixation and staining. The AGU fibroblasts exhibited polyploidy, (**Figure 12**) which was not seen in the healthy fibroblasts nor in either cell line in lower passages. Polyploidy was observed within cells after 30^{th} passage, but only in AGU fibroblasts.

In addition, healthy and AGU fibroblasts differed in an increase in cell size in AGU cells compared with the healthy cells. This can also be seen from **figure 12**, where healthy fibroblasts exhibit a homogenous cell population in terms of size and organization, but the AGU cells, in addition to polynucleated, also significantly enlarged.

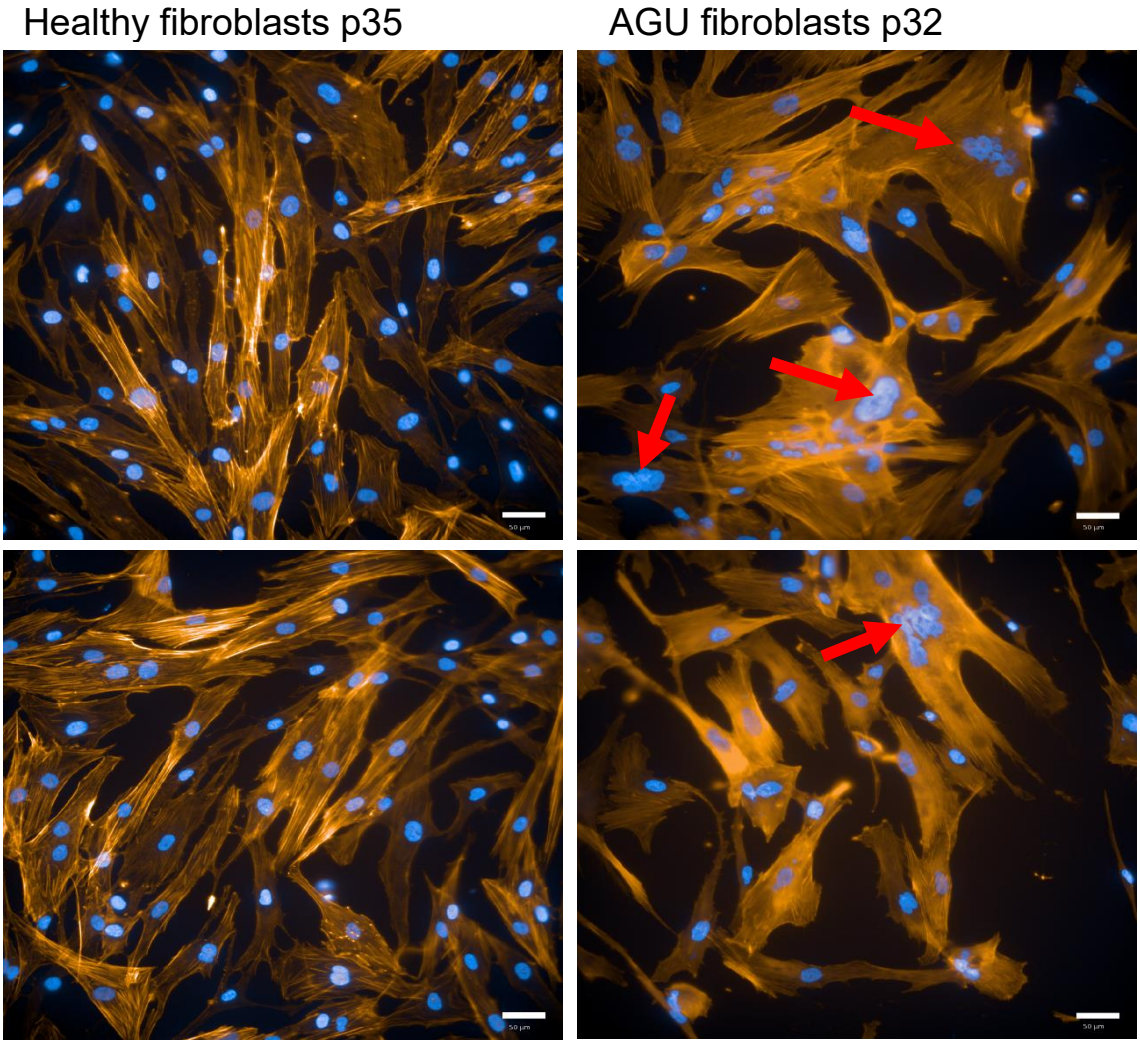

Figure 12. Different phenotype in AGU cells with higher passage. High passage AGU fibroblasts exhibit multinucleated cells (arrows) and enlargened cytoplasm, which is not seen in healthy fibroblasts even in high passages. Nucleus stained with DAPI (blue) and cytoskeleton with phalloidin (orange). Scale bar 50 µm.

3.4.4 TFEB staining

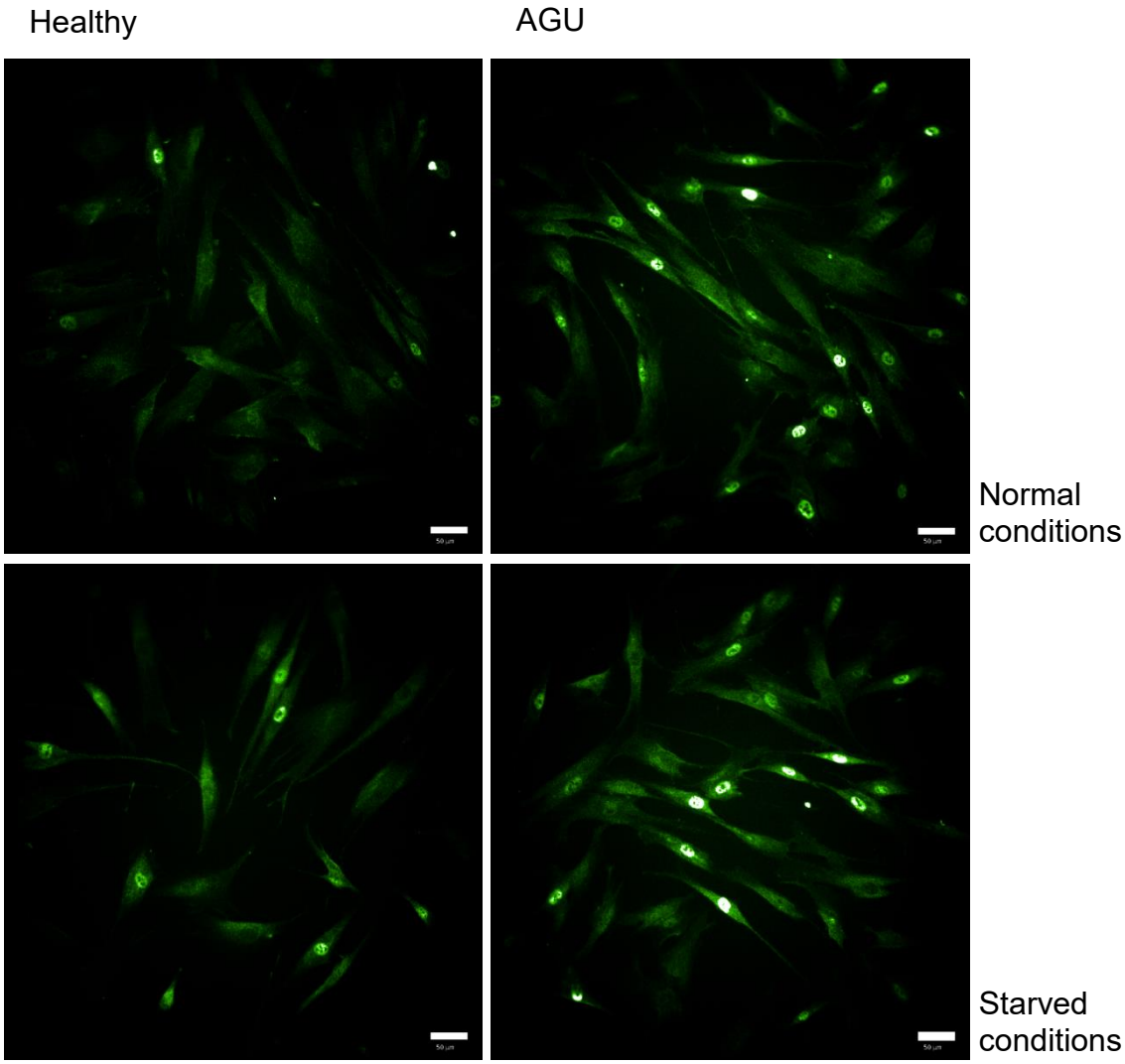

Figure 13. TFEB localization under normal and starved conditions. In AGU fibroblasts, TFEB is in nucleus in both starved and non-starved conditions, whereas in healthy cells the change in the culturing conditions and following relocation into the nucleus in response to starvation is more evident.

Both AGU and healthy fibroblasts were immunostained with anti-TFEB antibody to study the localization of TFEB in response to starvation. (**Figure 13**) The cells were starved for two hours in growth medium depleted of both serum and non-essential amino acids. After starvation, the cells were fixed and stained with anti-TFEB, phalloidin and DAPI. Nuclear TFEB signal was present in both starved and non-starved AGU cells, whereas only the starved healthy cells exhibited nuclear localization of TFEB. This suggests that there are

differences in TFEB phosphorylation regulated by mTOR between the AGU and healthy cells, which is seen in constant activation of TFEB. Under normal conditions, as in healthy cells, TFEB remains in its phosphorylated inactive state within the cytosol and is only activated by cellular stress.

3.5 Western Blotting

The expression and amount of the enzyme AGA within the AGU and control cells was studied with Western Blot. Three different antibodies were tested, and vinculin was used as the loading control. All three antibodies recognized the protein and right size bands were formed, but after optimization and based on the intensity of the signal, abcam anti-AGA was chosen for further experiments.

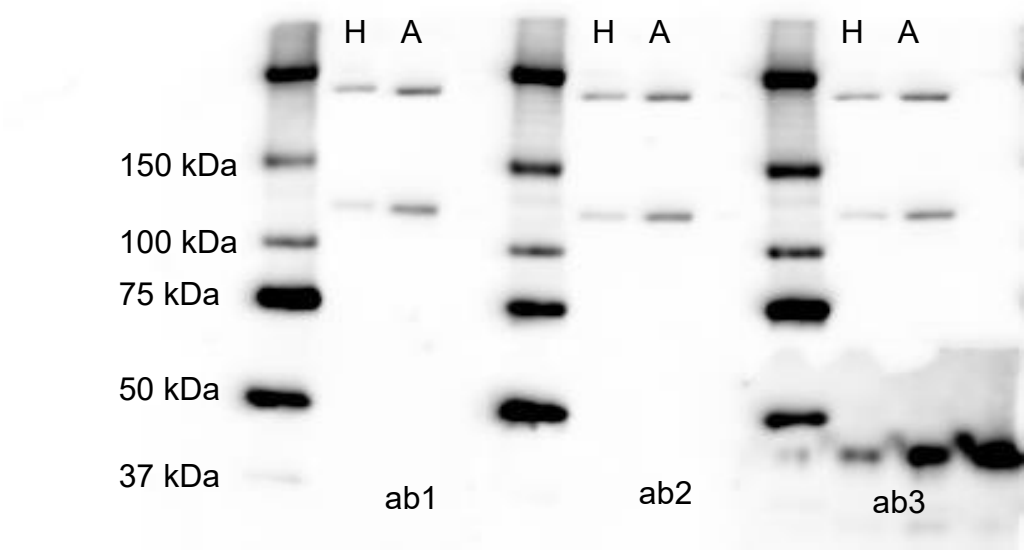

Figure 14. Antibody test with three different anti-AGA (42 kDa) antibodies. Vinculin (124 kDa) used as a loading control. Only ab3 recognized AGA with 1:1000. A third band is seen at ab3 due to spillage from AGU sample and a bigger, unspecific band at >150 kDa. H=Healthy, A=AGU, ab1=Novus Biologicals (NBP1-79881) ab2= Novus Biologicals (NBP1-88866), ab3= Abcam (ab231021).

In **figure 14**, the differences between the intensity of the signal from the three antibodies can be seen. Only Abcam antibody recognized the AGA enzyme

peptide with the 1:1000 dilution, which was recommended by all three antibody suppliers. The recognized AGA bands can be seen at 42 kDa in **figure 14**. In addition, a third band can be seen in addition to the healthy and AGU cell lysate due to spillage from the well of the AGU lysate. A bigger band at over 150 kDa can be seen, and this is due to unspecific binding of the anti-vinculin antibody. Based on this result, Abcam antibody was chosen to future Western Blot analyses.

After choosing the antibody, further Western Blotting experiments were conducted with different amounts of protein: 50 µg/ml, 75 µg/ml and 100 µg/ml. We wanted to compare the differences in the enzyme levels in healthy and AGU lymphocyte lysates with the Abcam antibody, which proved to give the most intense bands. In **figure 15**, the differences in the intensity of the bands between cell lysate from healthy and AGU lymphocytes can clearly be seen. The healthy lymphocytes exhibit bands of smaller intensity when comparing to the AGU lymphocytes, with all three different loaded protein amounts tested. The biggest intensity difference is seen with a band approximately 42 kDa in size, where AGU lymphocytes show a much clearer band compared with the healthy cell lysate. The most intense band is the size of the uncleaved enzyme, which is given by the antibody manufacturer as the recognized size. The intensity of the AGU cell lysate band is 2.26 times higher than the intensity of the band for healthy cell lysate when normalized with the loading control intensity, thus, there is 2.26 times more uncleaved AGA enzyme within the AGU cells compared with the healthy cells.

This suggests that the enzyme production itself is not impaired within the AGU lymphocytes, but the cleavage of the enzyme into its two subunits does not occur as in the healthy state. Thus, the AGU_{FIN} major mutation that is present in the AGU lymphocytes prevents the cleavage and formation of the active AGA enzyme, but not the transcription or translation of the peptide chain itself.

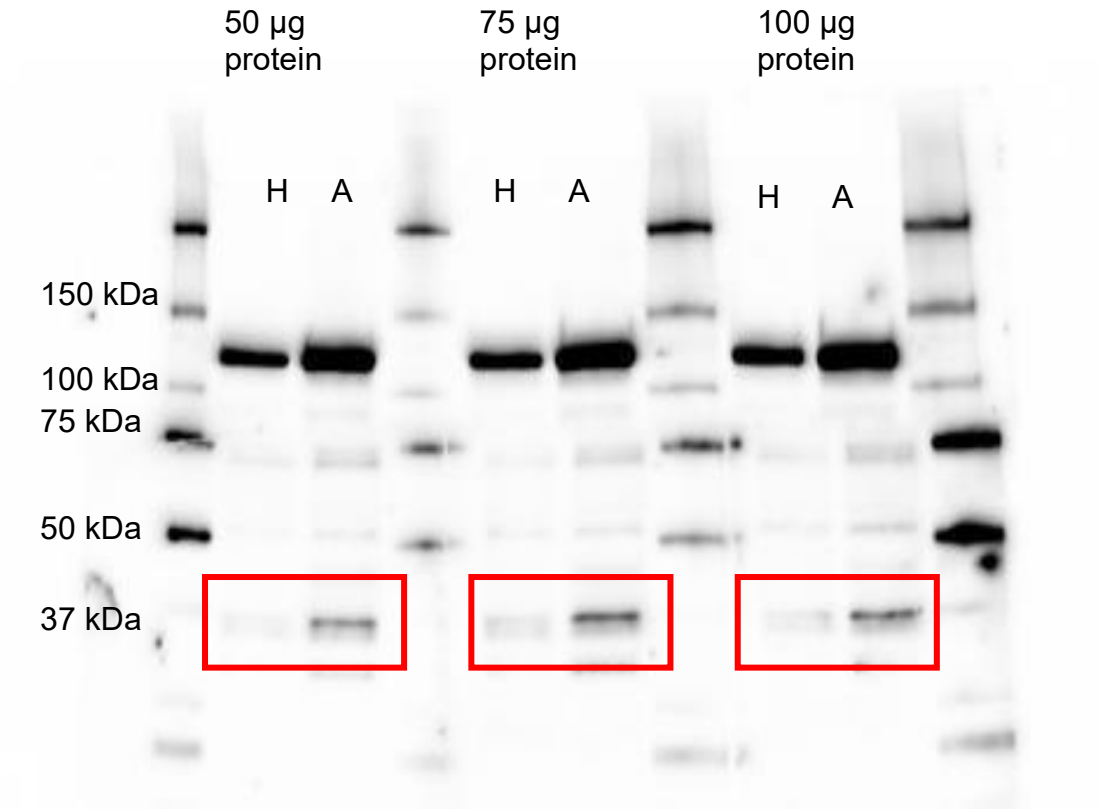

Figure 15. A dilution series of loaded cell lysate. A dilution series with 50, 75 and 100 µg of loaded protein show a stable 2.26 times higher AGA precursor amount in AGU lymphocyte lysate compared with the healthy cells (marked with red) when normalized with vinculin band intensity. Vinculin (124 kDa) was used as loading control. H=Healthy, A=AGU.

4. Discussion

4.1 Cell maintenance

Fibroblasts from an AGU patient and an age- and gender-matched control showed very different characteristics both morphologically and growth-wise. Since the growth pace for the AGU fibroblasts was very slow, the serum concentration was altered by increasing the FBS concentration from 15% to 20% as the cell supplier had suggested in their instructions. Despite these alterations, the AGU and healthy cells continued to differ in their growth rates. Interestingly, when comparing the different cell types for this phenomenon, the lymphocytes behaved differently. No differences in the growth rate were seen between the AGU patient lymphocytes and their age- and gender-matched healthy controls. Both cell lines grew consistently even when growing passages and the sub-culturing rate was the same for both AGU and healthy cells. Morphologically, the lymphocytes showed no differences when observing them under a microscope. No previous studies could be found which would have reported the morphological characteristics of these primary cell types, even if multiple studies have been conducted with these cell lines. (Fisher & Aronson, 1991; Mononen *et al,* 1991; Greco *et al,* 2003; Sarkar *et al,* 2018)

These findings support the decision to have at least two different cell types grown and investigated parallel to each other in case of cell-type specific problems occur. Since the four cell lines were obtained from four different individuals, the two different AGU cells' growth rate compared with their healthy controls might be due to the differences in the individuals the cells originate.

When the cell culture continued, the AGU fibroblasts started to show distinct morphological differences compared to the healthy fibroblasts. Observing the cell cultures under a microscope, the cells showed a significantly different phenotype. AGU patient cells had cell debris and significant number of dead cells in their growth medium after each subculture, compared with the healthy

fibroblasts. These differences might be caused by the poor attachment of AGU cells to the culturing vessel, which causes the cells to lose the natural growth condition and to undergo cell death. The debris might also originate from the unattached dead cells. Poor attachment might also be the cause for the poor growth rate, when a significant proportion of the sub-cultured cells does not survive. Although fibroblasts growing *in situ* are a very quickly renewable cell type, in primary cell culture, the poor attachment may be the underlying cause for poor growth. The differences are contrary to the findings of Näntö-Salonen and Penttinen (1982). They studied primary fibroblast cultures from skin biopsies of AGU patients and a healthy age- and gender matched controls under similar growth conditions and passages as the cells grown in this study. The group analyzed the cells for their growth rate and saw no differences between the AGU and healthy controls. Although same growth rates, Näntö-Salonen and Penttinen found that the synthesis of collagenous proteins was decreased in AGU cells compared with the healthy controls. Skin-affecting symptoms have also been reported in AGU patients by Arvio *et al* in 1999.

4.2 Enzyme activity measurement

The AGA enzyme activity measurements from the healthy and AGU cell lysates show a stabile enzyme activity in both cell lines, although in AGU cells the enzyme activity is below the sufficient activity needed for the cells to function adequately, being about 1/10 of the activity of the healthy cells. These baselines measured for both cell lines can now be used in future experiments as reference when comparing the enzyme levels between, for example, different treatment options.

Enzyme activity measurement for the commercially available recombinant enzyme showed that 1 µg/ml of enzyme exhibited enzyme activity by cleaving the substrate accumulated within the cells. This suggests, that in theory, the recombinant enzyme could be used to replace the inactive enzyme in AGU cells and that, with the right concentrations, the enzyme activity could be increased to sufficient levels also in the AGU cells. This was proven to work in

the lymphocyte culture: adding the recombinant enzyme to the culturing media increased the enzyme activity within the AGU cells by being able to decrease the amount of the enzyme substrate accumulation within the cells. Adding recombinant enzyme to the cell culturing media proved that the enzyme is endocytosed at an appropriate rate and that the enzyme activity remains high enough for the breakdown of the metabolic product for at least four days. The endocytosis happens probably via the MPRs located on the cell surface, and this allows the transportation of the enzyme to the lysosomes. Since the enzyme is a lysosomal enzyme, it requires an acidic environment in order to break down the substrates. Since the functionality was detected, it can be concluded that the enzyme is indeed transported to the lysosomes and remains intact for at least the now studied four days. In addition to this, it can be concluded that the acidic environment is preserved in the lysosomes also in the AGU states, based on the enzyme function. In addition, the LysoTracker DeepRed staining supported this by recognizing specifically the acidic environment of the lysosomes and endosomes. Thus, at least in AGU, the pathophysiology is not directly affecting the acidification of the lysosomes. This acidification process occurs through the V-ATPase located on the lysosomal membrane (Ohkuma *et al,* 1982), as discussed before. In addition to the V-ATPase, the lysosomal membrane enables the normal function by protecting the acidic environment from getting into contact with the cytosolic compartments (Alberts *et al,* 2015). In consideration with the results obtained, it can be stated that the acidification process and the protective membrane are functional enough to not be the underlying cause for the pathology in the AGU cells.

Of course, there are several different factors that need to be considered before these theories can fully be implemented to the pathophysiology of the lysosomal storage diseases. For example, regarding the endocytosis rate for the recombinant enzyme, there are multiple different factors that needs to be taken into account. Further studies are needed to investigate further e.g. the presence and exploitation of MPRs in physiological conditions and the level of the enzyme activity in cell culture conditions. However, an increase in enzyme function and decrease in the quantity of accumulated protein of this magnitude

with only 1 µg/ml of protein suggests, that treatment with a corresponding amount in humans, 1 mg/kg, could be possible in theory.

4.3 LysoTracker time point analysis

LysoTracker time point study with healthy fibroblasts, AGU fibroblasts, starved healthy fibroblasts and starved AGU fibroblasts was conducted over an 18-hour period and the cells were imaged every 20 minutes. The differences between the groups are most evident from 2 hours up to 8 hours. This suggests that after the depletion of serum from the growth media, it takes at least two hours for the autophagic machinery to start the degradation process when deprived of nutrients. Since the autophagy is thought to continue for longer than three hours from its imageable peak, the decrease in signal intensity might be caused by the fading of the fluorescent label of the LysoTracker due to tens of exposures to light after numerous images and the initial dilution protocol of the LysoTracker.

The decrease of the fluorescent signal may also be due to the alkalizing effect of the LysoTracker, which causes the signal to weaken since the probe is activated by the acidic environment of the organelles. Indeed, this must be considered when interpreting the results, but for future experiments, this should not play a significant role since the cells are not to be imaged for extensive periods.

Based on these findings, further optimization for starvation was performed after the time series study. In future experiments, the LysoTracker label was introduced to cells after 5.5 h of starvation for the imaging to take place at 6 hours from the nutrient deprivation initiation. The starvation conditions were also altered by fully depleting the FBS from the growth medium of the cells in contrast to the timepoint study, where growth medium containing 5% FBS was used. In future experiments, the LysoTracker is a useful tool to image the lysosome activity within the cells. Although LysoTracker is not lysosome specific as it stains according to the low pH of the vesicles and thus may

recognize also late endosomes, it is still a convenient probe for lysosomal studies.

4.4 Starvation and immunofluorescent staining

Several 96-well plates were studied combining the starvation, LysoTracker labelling and antibody staining for fixated cells. The primary aim was to study the distribution of the lysosomes in starved cells compared with the healthy nonstarved fibroblasts, and to compare these with the AGU fibroblasts under starved and normal conditions. LAMP-1 recognizing antibody was used to compare the lysosome staining specificity between LAMP-1 antibody and LysoTracker.

In a study conducted by Banning *et al* in 2016, patient fibroblasts from the same AGU-patient as in this study were stained with LAMP-1 and LysoTracker together with a control fibroblast from a different source. These results are conflicting with our immunostaining results in terms of the lysosome amounts in the patient and control fibroblasts. In the study by Banning *et al,* the LAMP-1 and LysoTracker stained organelles were significantly more numerous than in the healthy fibroblasts, and this difference was not as profound in our study. These differences may be due to the differences in the healthy control fibroblasts, since they were obtained from a different source. The stainings were probably also done with different passages, although the passages of used cells were not revealed in the Banning *et al* study. The cells were cultured under different culturing conditions, which might also play a role, although since both the healthy and AGU cells were in same conditions in both studies, this should not affect the differences between the specific cell lines. In future studies, this staining should be repeated in mimicked conditions from Banning *et al* study, after which further conclusions from the reasons behind observed differences between the studies could be drawn.

The small co-localization percentages were probably due to the different properties of the probes. LAMP-1 is a surface protein expressed on the lipid

layer of lysosomes and is also found on the lipid layer of late endosomes. In addition to this, it must be considered that antibodies behave differently than a chemical probe. There is always a possibility of unspecific binding, although commercially available antibodies should be relatively specific. Indeed, these factors must be considered when analyzing the results of the staining. On the other hand, LysoTracker stains according to the acidic environment within the lumen of the cellular organelles, and lysosomes are not the only organelles exhibiting a decreased pH. In addition to lysosomes, also late endosomes have an acidic lumen and thus, none of these methods can fully differentiate the lysosomes from their predecessors.

Based on the comparison of the antibody and LysoTracker colocalization, LysoTracker was chosen for future experiments due to the higher percentage of overlapping with LAMP-1 than what LAMP-1 overlapped with LysoTracker. In addition, LysoTracker is easily and reliably repeatable and offers the possibility to use more immunofluorescent probes due to its infrared wavelength.

The second staining of fibroblasts in a similar setup as the LAMP-1 and LysoTracker comparison yielded different results. The cells were starved, incubated with LysoTracker and stained with phalloidin and DAPI, in order to analyze the distribution of the lysosomes. Due to the significantly different phenotypes of the already older cells between healthy and AGU, no analysis could be conducted since the validity of the results could not be guaranteed. The AGU fibroblasts were notably bigger in size, and many of the cells had multiple nuclei or a nucleus that was scattered, not uniform, and did not exhibit a round shape as like healthy cells. In addition to this finding, the healthy cells grew in an organized manner, and the AGU cells were scattered disorderly as seen in **figure 3**, in chapter 3.1 Cell Maintenance and **figure 12** in chapter 3.4.3 Starvation.

The abnormality of nuclei in AGU fibroblasts is possibly due to either cell fusion or an aborted mitosis, where nucleus is divided but the mitosis process is not advanced further to full cell mitosis. In macrophages, multinucleated cells can form also via phagocytosis. (Hornik *et al,* 2014) In a study conducted by Sukita

et al in 2019 multinucleated cells were produced by incomplete mitosis. *Xenopus* tadpole epithelium tissue-derived cell line (XTC-YF) was used to investigate conditions under which multinucleated cells form. The group altered the surface hydrophilicity of the cell culture surfaces, which makes the results not completely applicable with our results. Since the phenomenon was seen after immunofluorescent staining, it can only be stated that fibroblasts exhibited polyploidy due to no staining of lymphocytes.

Since this phenomenon is not detected in the healthy fibroblasts, it can be hypothesized that the impaired lysosomal function is at least partially causing the atypical nuclei. Arvio *et al* (1999) reported facial angiofibromas and erythema and seborrhoeic skin to be more frequent in AGU patients than in general population. However, *in vitro* growth conditions are incompatible with the normal multicellular tissue conditions. The unorganization of the AGU fibroblast cell culture might be the *in vitro* equivalent to the skin symptoms reported by Arvio *et al* in 1999.

In 2018, Samarani *et al* reported of cell cycle arrest coupled with abnormal lysosomal function. The group induced LSD-mimicking conditions by loading lysosomes with sucrose, commonly used to impair lysosomal function and study the consequences. Decrease in proliferation rate, increase in apoptotic cells and downregulation of cell cycle regulating genes was observed. However, the findings by Samarani *et al* cannot directly explain the atypical nuclei discovered in the AGU patient cells when staining with DAPI. Cell growth arrest may explain the splitted nucleus, if cell undergoes mitosis up until the splitting of cytoplasm, which is not completed because of downregulated genes regulating the cell cycle. This remains to be studied in the future.

A second starvation experiment was conducted with fibroblasts, similar to the previous experiment with LysoTracker DeepRed and LAMP-1 staining, and with cells with smaller passage. The cells were depleted of FBS for 16 hours, after which they were stained with LysoTracker, phalloidin and DAPI. The cells were imaged, and the images were analyzed by the distribution of lysosomes peripherally or perinuclearly. There was a significant increase in the

perinuclear intensity of the LysoTracker when the cells were starved, compared with the non-starving conditions. This can be explained by the autophagic machinery reacting to the absence of nutrients. The cellular stress caused by the deprivation of nutrients triggers the relocation of TFEB into the nucleus, which results in transcriptional activation of genes regulating autophagy and lysosomal biogenesis. This lysosomal biogenesis can be seen from the images obtained after the starvation experiment, in an increased signal within the perinuclear area (**Figure 11**). In line with this result is the increase in nuclear TFEB signal in immunostaining. TFEB is the transcriptional activator of lysosomal proteins required for lysosome biogenesis in response to nutrient deprivation. This biogenesis starts when TFEB is activated and relocates into nucleus, as seen from the immunostaining (**Figure 13**) images. In AGU cells in contrast, TFEB is located in the nucleus even under non-starved conditions. In 2009, Sardiello *et al* demonstrated the nuclear relocation of TFEB in response to lysosomal stress in HeLa cells after sucrose supplementation, which is commonly used to mimic lysosomal stress and lysosomal storage diseases. Since AGU cells exhibit TFEB localization in nucleus under both starved and non-starved conditions, it can be thought that TFEB signaling route is not impaired *per se.* However, regardless of TFEB localization within the nucleus the effect of its active state is not seen as an increase in lysosomes in AGU cells. When reflecting on the non-starved conditions in lysosome localization study and comparing with healthy cells the lysosomes of AGU cells are not closer to the nucleus nor is the perinuclear lysosome amount increased. Thus, even if TFEB relocates to the nucleus the effects of it are not seen as would be expected: as an increase in lysosome biogenesis.

It is interesting to speculate the connection between AGU, or LSDs in general, and the preliminary TFEB differences seen in immunofluorescent staining. Actually, lysosomal storage disorders and overexpression of TFEB have been studied together from an enhanced exocytosis and autophagy point of view. Various lysosomal storage diseases have been proved to exhibit a decrease in the accumulated metabolic byproduct when TFEB is overexpressed. (Medina *et al,* 2011; Spampanato *et al,* 2013; Song *et al,* 2014) These studies

support the hypothesis of a functioning TFEB signaling pathway in lysosomal storage diseases, which may be suitable for therapeutic aspects in the future.

In future experiments, it would be interesting to replicate these studies with another LSD primary cell line to study if the pathological state affects e.g. the aging cells similarly. In addition, the TFEB and lysosome localization studies would be intriguing to replicate in order to see if the differences between healthy and LSD cells remain. From therapeutic aspect, it would be beneficial if pathological similarities would be found and the LSDs could share a therapeutic approach.

4.5 Western Blot

Western blot analysis with anti-AGA antibody showed an increased expression of AGA in the AGU lymphocyte cell lysate. Aspartylglucosaminidase, the lysosomal enzyme responsible of the metabolism of aspartylglucosamine in healthy cells, is not functional in the AGU cells despite the increased expression. Under normal conditions, the enzyme is autocatalytically cleaved into its two subunits, which form the active heterotetrameric AGA-enzyme consisting of two alpha and two beta chains. These subunits are at 24-205 aa (alpha) and 206-346 aa (beta) with a signal peptide preceding the subunits. The anti-AGA antibody is reported to recognize the amino acids 28-245 of the human enzyme, of the total 346 amino acids (UniProt.org, P20933). Thus, the antibody recognizes the enzyme before it is cleaved into the subunits, which can be the underlying cause to the seemingly higher protein expression in the AGU cells lysates. This result is in line with the fact that the malfunctioning enzyme accumulates within the cell causing downstream effects in its secondary substrate accumulation and damaging the overall cellular function (Schultz *et al,* 2011).

In future experiments, antibodies that recognize the different subunits should be used in addition to the one recognizing the entire amino acid chain.

4.6 Study Limitations and Conclusions

The limitation of this study is the narrow patient population in terms of the origin of the cells used. Although both of the patient cells carry the most common mutation (AGU_{FIN} major), it must kept in mind that there are other mutations within the *AGA* gene causing AGU. However, from a drug discovery perspective, the established patient model is good enough for a baseline, which can then be altered to aim for the baseline of the healthy cells, as long as the limitations are kept in mind. Additionally, future studies are needed with other LSD types before wider exploitation and generalization of these results to cover other LSD pathologies.

As a conclusion, the characterization of the cells produced a valid efficacy model for future studies with various modalities within the Therapy Area Rare Diseases at Orion Pharma Orion Corporation. The enzyme activity measurements distinguished the healthy cells with a sufficient AGA activity from the AGU cells with an enzyme activity diminished to approximately 10% of the healthy cells. Corresponding to these results, the GlcNAc-Asn amount in the healthy cells was significantly lower than in the AGU cells where accumulation of the substrate was seen. With Western Blot analysis, a bigger amount of an uncleaved proenzyme was seen in the AGU cells compared with the healthy cells, in which the enzyme was presumably more effectively cleaved into its subunits. In immunostaining experiments, no clear difference was seen in the lysosome localization between the healthy and AGU cells, and thus, this method is still in need for optimizing of better antibodies more reliably recognizing lysosomal markers. TFEB staining, however, yielded interesting differences between the healthy and AGU cells in the subcellular localization and thus active state of TFEB. These optimized methods to model lysosomal storage diseases now allow the full utilization in studying the intervention options for numerous lysosomal storage diseases and thus may in the future play a role in alleviating the symptoms in patients affected.

5. Materials and methods

5.1 Cell culture

Fibroblasts were attained from Coriell Institute (New Jersey, USA). Aspartylglucosaminuria cells (GM00568) were from an 18-year-old female patient of Finnish origin, and the control cells (GM03651) used were gender- and age matched control (Female, 25 years old, Caucasian). AGU fibroblasts were cultured in Eagle's Minimum Essential Medium (EMEM) with Earle's salts supplemented with non-essential amino acids (NEAA), PenStrep, 20% Fetal Bovine Serum (FBS) and GlutaMAX. Control fibroblasts were cultured with the same medium and supplements, but only 15% FBS. Sub-culturing of the cells: Confluent cell culture vessels were washed with 1X DBPS (Dulbecco's phosphate-buffered saline) and incubated with 0.25% Trypsin until the cells detached. Medium was used to inactivate the trypsin before centrifugation (110 g for 10 minutes at RT). The cells were reseeded at approximately $1.0*10^4$ cells/cm^2 once or twice per week in Nunc™ T75 cell culture vessels. Refer to **table 1** for details of materials used in cell culture.

Lymphoblasts were attained from Coriell Institute (New Jersey, USA). Cells from healthy individual (GM07521, 19 years old, Female, Caucasian) and AGU patient (GM10417, 14 years old, Female, Caucasian (Finnish)) were both grown in RPMI 1640 medium with L-Glutamine supplemented with PenStrep and 15% FBS. The cells growing in suspension were reseeded at approximately $2*10^5$ cells/ml twice per week in Nunc™ T25 cell culture vessels.

Detaching the fibroblasts for sub culturing proved to be very inefficient with the instructions provided by the supplier. The protocol was optimized with 0.04%, 0.08%, 0.16% and 0.25% trypsin in 0.53 mM EDTA in HBSS. Different detachment methods were tested parallel to make sure the phenotype of the cell culture was not altered. In addition to the detachment methods, different culture vessels with different coatings were tested. Based on the outcomes

after four weeks of parallel culture methods, a DPBS wash prior to detaching the cells with 0.25% trypsin was introduced.

Table 1. Materials used in cell culture

Material	**Supplier**	**Catalog #**
DPBS	Gibco™, ThermoFisher Scientific	14190-094
EMEM Cell Culture Medium	Sigma-Aldrich	M2279-500ML
EDTA (Ethylenediaminetetraacetic acid)	Sigma-Aldrich	60-00-4
FBS	Sigma-Aldrich	F7524
GlutaMAX™	Gibco™, ThermoFisher Scientific	35050-038
HBSS	Gibco™, ThermoFisher Scientific	14065-049
MEM NEAA	Gibco™, ThermoFisher Scientific	11140-035
Nunc™ EasYFlask™ 75 cm^2 Nunclon™ Delta Surface	ThermoFisher Scientific	156499
Nunc™ EasYFlask™ 25 cm^2 Nunclon™ Delta Surface	ThermoFisher Scientific	156367
PenStrep	Gibco™, ThermoFisher Scientific	15140-122
RPMI-1640	Gibco™, ThermoFisher Scientific	A10491-01
Trypsin (0.5% Trypsin-EDTA)	Gibco™, ThermoFisher Scientific	15400-054

5.2 Starvation

Starved cells were used in immunofluorescent imaging and LysoTracker time series experiment. The fibroblasts used for these experiments were plated at least one day prior to starting the study with a confluency of 5000 cells / well on a tissue culture 96-well plate treated with a tissue culture (TC) -coating (CellCarrier™-96 Ultra, PerkinElmer, 6055300). The normal growth medium was removed by aspiration and the pre-heated starvation medium (normal medium depleted of FBS, containing either 0% of 5% FBS, depending on the study) was pipetted onto the cells. Control cells were treated similarly. Starvation medium was supplemented with GlutaMAX, NEAA and PenStrep at all times, excluding the TFEB staining, where the media was deprived of NEAA in addition to FBS.

5.3 Cell lysate for enzyme activity measurement

Cell lysates were prepared from both AGU and healthy lymphocytes. Approximately 60 million cells were centrifuged for 10 minutes x 120 g at RT. The pellet was resuspended in approximately 500 ul of 0.1% TritonX-100 (Triton™ X-100, Sigma-Aldrich, X-100-100ML) in DPBS. Three freeze-thaw cycles with vortexing were used to lyse the cells. The cell suspension was frozen on dry ice and then thawed in warm water bath coupled with vortexing. After freeze-thawing, the lysate was centrifuged for 10 minutes x 10 000 g at +4C. The supernatant was collected and stored in -20C until further analysis.

5.4 Enzyme activity measurement

Enzyme activity was measured from cell lysates from lymphocytes (described above). Tris-HCl buffer with 1% ethylene glycol (Sigma-Aldrich, 107-21-1) was used as buffer, pH adjusted to 7.5. L-Aspartic acid β 7-amido-4-methylcoumarin (Asp-AMC, Sigma-Aldrich, A1057) was used as substrate.

The substrate was weighted and diluted to DMSO to make 10 mM stock. The stock was further diluted to the buffer to make 800 µM working dilution. 7-Amino-4-methylcoumarin
(AMC, Sigma-Aldrich, 257370) was used as a standard. Standard was weighted and 50 mM stock was made in Dimethyl Sulfoxide (DMSO, Sigma-Aldrich, D2650-50ML).

¼ (25 µl) cell lysate or buffer, ¼ (25 µl) Asp-AMC or buffer and ½ (50 µl) buffer was pipetted onto a 96well plate (Cliniplate, ThermoFisher Scientific, 9502227). Dilutions of 1:2 starting from 1000 nM were used for standard curve establishment (200 µl per well).

Absorbance was measured with EnSpire™ Microplate Reader 23001365 with software EnSpire® 4.1. Baseline measurement was performed directly after substrate addition, excitation 360 and emission 460. The plate was kept covered in 37 C and enzyme activity was measured again after 24 hours.

The same method was used to measure the activity of a commercially available recombinant enzyme (Recombinant Human AGA Protein, Novus Biologicals, NBP2-52631). Tris-HCl buffer supplemented with 1% ethylene glycol was used as the buffer, Asp-AMC prepared fresh to DMSO was used as the substrate and AMC dilution series for the standard curve measurement. The recombinant enzyme was diluted to the buffer to make 10 µg/ml dilution, and further combined with 80% buffer, and 10% Asp-AMC, which was added just before measurement to make a final concentration of the recombinant enzyme to 1 µg/ml as highest. Dilution series for the recombinant enzyme was prepared to start from 1 µg/ml with 1:3 dilutions. The activity was measured with EnSpire™ Microplate Reader 23001365 with software EnSpire® 4.1. for two hours at RT, imaged every two minutes with shaking in between the measurements. Excitation of 360 nm and emission of 460 nm was used for all enzyme activity measurements.

Km values of AGA were defined for healthy lymphocytes with a substrate dilution series and a standard curve. 7-Amino-4-methylcoumarin (AMC, SigmaAldrich, 257370) diluted to DMSO to 50 mM was used as a standard and Michaelis-Menten equation was used to calculate the Km values.

Visual assessment and Shapiro-Wilk test were used to check the normality of data. After this, for all of the enzyme activity measurement results, two-sample t-test with assumption for normality was done to test for statistical significance. The same test was done in the analysis of GlcNAc-Asn amount, although normality could not be checked due to small number of replicates. P-value <0.05 was considered significant.

All calculations and figures were done with GraphPad Prism (8.0.2 (263)). Mean and SD shown on each graph.

5.5 Immunofluorescence

For immunofluorescence staining, the cells were washed 5 min with DPBS before fixation with 3.7% formaldehyde in DPBS for 20-30 minutes in RT. Sequentially, the cells were then washed twice with DPBS for 5 minutes followed by blocking in 10% FBS, 0.1% TritonX-100 or 1% saponin (Sigma-Aldrich, 8047-15-2), 1% Bovine Serum Albumin (BSA, Sigma-Aldrich, A2153-100G) in DPBS for 45-60 minutes in RT. After blocking, the cells were washed with 1% serum, 0.1% TritonX-100 or 1% saponin, 1% BSA in DPBS once before using the same solution in primary antibody mixture. Primary antibodies were incubated O/N in +4 C. Refer to **table 2** for antibody dilutions used.

The cells were washed three times 5 minutes with 1% BSA in DPBS. Secondary antibody was diluted to 1% BSA in DPBS and incubated on cells for 1 h in RT. Together with secondary antibody, Phalloidin was added onto the wells in order to detect the cytoskeleton. For the last 5 minutes, 1:1000 DAPI was added to the secondary antibody solution. After secondary antibody incubation, the cells were washed for 5 minutes each, 2-3 times with DPBS and 1-2 times with phosphate buffer (0.01 M NaH_2PO_4 and 0.01 M Na_2HPO_4 in dH_2O). The last wash was left on and the plate was imaged with Operetta CLS™, PerkinElmer, and with the Harmony software (PerkinElmer, 4.9.2137.273). The images were exported and analyzed with Columbus (Columbus, 2.8.2.1205, PerkinElmer).

When no primary antibodies were used for fibroblast staining, the protocol was started from the blocking after fixation of the cells, and the plate was washed once with 1% BSA in DPBS before incubations with phalloidin and DAPI. Washing and imaging the plate was done as when using primary antibodies.

For statistical analysis of the positioning of lysosomes, normality of data was checked both visually and with Shapiro-Wilk test. For normally distributed data, one-way ANOVA was used to conduct statistical analysis for all sample groups. In cases data was not normally distributed, Mann-Whitney test was conducted and the groups were analyzed pair-wise. P-value <0.05 was considered significant.

Table 2. Antibodies and fluorescent stains used in immunostaining and Western Blot analysis.

Immunofluorescence antibodies				
Primary	Anti-LAMP-1	Novus biologicals	NB120-19294	1:500
	Anti-TFEB	Abcam	ab220695	1:500
Secondary	DAPI	Sigma-Aldrich	D9542	1 mg/ml, further diluted 1:1000 to wells
	Goat anti-rabbit Ig-G Alexa 488	InVitrogen	A11034	1:400
	LysoTracker™ Deep Red	InVitrogen	L12492	75 uM
	Phalloidin, Alexa Fluor® 568	InVitrogen	A12380	1:400
Western Blot antibodies				
Primary	Anti-AGA	Novus Biologicals	NBP1-79881	1:1000
	Anti-AGA	Novus Biologicals	NBP1-88866	1:1000

	Anti-AGA	Abcam	ab231021	1:1000
	Anti-Vinculin	Abcam	ab129002	1:10 000
Secondary	Goat anti-rabbit IgG-HRP	BioRad	#1706515	1:3000
	Precision Protein StrepTactin-HRP Conjugate	BioRad	#161-0380	1:5000

5.6 Cell lysate and protein measurement for Western Blot

Cell samples for western blot analysis were prepared by lysing the cells using MPER buffer (Thermo Fisher, #78501) supplemented with 4% protease inhibitor solution (Complete EDTA-free, Roche, #11873580001 in Milli-Q) and 10% phosphatase inhibitor solution (PhosSTOP, Roche, #04906837001 in M-PER buffer; Thermo Fisher, #78501).

Protein concentration of the cell lysates was determined with Micro BCA Protein Assay Kit (Thermo Scientific, #23235) according to the manufacturer's instructions. The luminescence was measured with EnSpire™ Microplate Reader 23001365 with software EnSpire® 4.1.

5.7 Western Blot

Western blot samples were prepared for the polyacrylamide gel electrophoresis by thawing the samples on ice. Then 4 x Laemmli loading buffer (BioRad #1610747, completed with 10% β-mercaptoethanol) and an appropriate amount of Lysis buffer was pipetted to an Eppendorf tube together with an appropriate amount of the cell lysate to equal 30 µg of protein per well.

The samples were boiled at 95 C for five minutes and centrifuged 10 000 x g for 10 s.

7 µl of MW standard (BioRad, Precision plus protein™ WesternC™ Blotting Standards, #161-0376) and 40 µl of samples were pipetted to the gel (BioRad Criterion TGX Stain-free 4-15%, #5678083) after filling the running chamber and rinsing the wells with 1 X Tris/Glysine/SDS buffer (BioRad, #161-0772). The gel was run with 100-120V for 60-120 minutes, until the smallest samples were at the bottom of the gel.

After the run, the gel was transferred to transfer buffer and onto the blotting membrane (BioRad Trans-Blot Turbo Midi Nitrocellulose, #1704159) and after constructing the sandwich, blotted with Trans-Blot Turbo Mixed MW>150, for 7 minutes. After blotting, the membrane was cut to appropriate sizes for continuation with antibody staining.

The membrane was blocked in 5% milk (Blotting Grade Blocker, BioRad, 1706404), 0.1% Tween-20 in 1 X TBS (TBS Tween™-20, ThermoFisher Scientific, 28360) for 1 h on a tilter.

Primary antibody was diluted to the blocking buffer and the membrane was incubated O/N in +4 C on a tilter. Refer to **table 2** for antibodies and dilutions used.

After primary antibody incubation, the membrane was rinsed trice with TBST and washed 3 x 5 minutes on a tilter in RT. The secondary antibody dilution was made in the same buffer as the primary antibody dilution. Wash solution was removed before addition of the secondary antibody dilution (Goat anti-rabbit IgG-HRP, BioRad, #1706515, 1:3000) and StrepTactin (Precision Protein StrepTactin-HRP Conjugate, #161-0380, 1:5000), and the membrane was incubated for 1-2 h on a tilter, protected from light at RT.

The membrane was then rinsed 3 x and washed 3 x 5 minutes with TBST on a tilter, protected from light at RT. ECL (BioRad #1705061) 1:1 was used for detection: excess buffer was dried off membrane and ECL was pipetted onto the membrane. The membrane was incubated 2 minutes protected from light and imaged with Azure Biosystems c400 and cSeries Capture Software 1.9.2.0315.

The band intensity was determined with ImageJ software version 1.52a (Wayne Rasband, National Institutes of Health, USA). The target protein/loading control ratio was determined for both healthy and AGU AGA bands. The ratio was further normalized to the intensity of the band of healthy cells, which could be used to determine the increased intensity for the AGU cell band.

5.8 LysoTracker

Lysosomes were labelled with LysoTracker DeepRed (InVitrogen, #L12492). The 1 mM stock was diluted to cell growth medium to make a 10 µM working stock. This stock was further diluted to growth medium to the desired dilution of 75 nM. Growth medium of the plated cells was aspirated and pre-warmed medium with dye was pipetted onto the cells with as little light as possible. The cells were incubated with the dye in 37°C for 30 minutes after which the medium was changed. The plates were then either imaged with appropriate excitation and emission wavelengths for the dyes or the plate was fixed and stained according to the chapter 7.5 above.

6. Acknowledgements

I want to sincerely thank my supervisors Riikka Äänismaa and Jarkko Venäläinen for supporting me and guiding me through this thesis project. They have selflessly given time to my thesis regardless of their own projects and always answered to my questions with expertise. In addition, I want to thank the colleagues in Therapy Area Rare Diseases and other departments in Orion Corporation Orion Pharma for their help, answers to my questions and their time. I am lucky to be surrounded by such a talented team. Especially essential help has been received from Simo Vainionpää, thank you for keeping my cells alive.

Without my amazingly bright friends and motivating teachers, this would not have happened. Thank you for peer pressure and everlasting encouragement throughout these memorable university years. Lastly, I want to thank my biggest supporters, the family. Thank you for always believing in me and for lifting me to heights I did not know I could reach. You are my inspiration.

7. Abbreviations list

AGA	Aspartylglucosaminidase
AGU	Aspartylglucosaminuria
BBB	Blood-Brain Barrier
BMT	Bone Marrow Transplantation
CI-MPR	Cation-Independent Mannose-6-Phosphate Receptor
CLEAR	Coordinated Lysosomal Expression and Regulation
CNS	Central Nervous System
CD-MPR	Cation-Dependent Mannose-6-Phosphate Receptor
EE	Early Endosome

EMA	European Medicines Agency
ER	Endoplasmic Reticulum
ERT	Enzyme Replacement Therapy
FDA	U.S. Food and Drug Administration
GlcNAc-Asn	Aspartylglucosamine
IGF-II	Insulin-like Growth Factor Receptor
LAMP-1	Lysosome Associated Membrane Protein 1
LE	Late Endosome
LSD	Lysosomal Storage Disease
M6P	Mannose-6-phosphate
MPR	Mannose-6-phosphate receptor
mTOR	Mechanistic Target of Rapamycin
SNARE	N-ethylmaleimide-Sensitive Factor-Attachment Protein Receptor
SRT	Substrate Reduction Therapy
TFEB	Transcription Factor EB
TGN	Trans-Golgi-Network
V-ATPase	ATP-Dependent vacuolar proton pump

8. References

Alberts, B., A. Johnson, J. Lewis, D. Morgan, M. Raff, K. Roberts, and P. Walter. 2015. Molecular Biology of the Cell. Garland Science, New York, US. 695 pp.

Arvio, M. 1993. Follow-up in patients with aspartylglucosaminuria. Part I. The course of intellectual functions. *Acta Pædiatrica.* 82:469-471. doi: 10.1111/j.1651-2227.1993.tb12725.x.

Arvio, M., V. Oksanen, S. Autio, E. Gaily, and K. Sainio. 1993. Epileptic seizures in aspartylglucosaminuria: a common disorder. *Acta Neurologica Scandinavica.* 87:342-344. doi: 10.1111/j.1600-0404.1993.tb04114.x.

Arvio, M.A., J.M. Rapola, and P.M. Pelkonen. 1998. Chronic arthritis in patients with aspartylglucosaminuria. *The Journal of Rheumatology.* 25:1131-1134.

Arvio, M., O. Sauna-aho, and M. Peippo. 2001. Bone marrow transplantation for aspartylglucosaminuria: Follow-up study of transplanted and non-transplanted patients. *The Journal of Pediatrics.* 138:288-290. doi: 10.1067/mpd.2001.110119.

Arvio, M.A., M.M. Peippo, P.J. Arvio, and H.A. Kääriäinen. 2004. Dysmorphic facial features in aspartylglucosaminuria patients and carriers. *Clinical Dysmorphology.* 13:11-15. doi: 10.1097/00019605-200401000-00003.

Arvio, P., M. Arvio, M. Kero, S. Pirinen, and P. Lukinmaa. 1999. Overgrowth of oral mucosa and facial skin, a novel feature of aspartylglucosaminuria. *Journal of Medical Genetics.* 36:398-404. doi: 10.1136/jmg.36.5.398.

Bai, X., D. Ma, A. Liu, X. Shen, Q.J. Wang, Y. Liu, and Y. Jiang. 2007. Rheb Activates mTOR by Antagonizing Its Endogenous Inhibitor, FKBP38. *Science.* 318:977-980. doi: 10.1126/science.1147379.

Bajaj, L., P. Lotfi, R. Pal, A.d. Ronza, J. Sharma, and M. Sardiello. 2019. Lysosome biogenesis in health and disease. *Journal of Neurochemistry.* 148:573-589. doi: 10.1111/jnc.14564.

Banning, A., C. Gülec, J. Rouvinen, S.J. Gray, and R. Tikkanen. 2016. Identification of Small Molecule Compounds for Pharmacological Chaperone Therapy of Aspartylglucosaminuria. *Scientific Reports.* 6:37583. doi: 10.1038/srep37583.

Banning, A., M. Schiff, and R. Tikkanen. 2018. Amlexanox provides a potential therapy for nonsense mutations in the lysosomal storage disorder Aspartylglucosaminuria. *BBA - Molecular Basis of Disease.* 1864:668-675. doi: 10.1016/j.bbadis.2017.12.014.

Beck, M. 2017. Treatment strategies for lysosomal storage disorders. *Developmental Medicine & Child Neurology*.60:13-18. doi: 10.1111/dmcn.13600.

Bootman, M.D., T. Chehab, G. Bultynck, J.B. Parys, and K. Rietdorf. 2018. The regulation of autophagy by calcium signals: Do we have a consensus? *Cell Calcium.* 70:32-46. doi: 10.1016/j.ceca.2017.08.005.

Bossi, G., S. Booth, R. Clark, E.G. Davis, R. Liesner, K. Richards, M. Starcevic, J. Stinchcombe, C. Trambas, E.C. Dell'Angelica, and G.M. Griffiths. 2005. Normal Lytic Granule Secretion by Cytotoxic T Lymphocytes Deficient in BLOC-1, -2 and -3 and Myosins Va, VIIa and XV. *Traffic.* 6:243-251. doi: 10.1111/j.16000854.2005.00264.x.

Boya, P., and G. Kroemer. 2008. Lysosomal membrane permeabilization in cell death. *Oncogene.* 27:6434-6451. doi: 10.1038/onc.2008.310.

Bucci, C., P. Thomsen, P. Nicoziani, J. McCarthy, and B. van Deurs. 2000. Rab7: A Key to Lysosome Biogenesis. *Molecular Biology of the Cell.* 11:467-480. doi:
10.1091/mbc.11.2.467.

Cawley, N.X., C. Sojka, A. Cougnoux, A.T. Lyons, E. Nicoli, C.A. Wassif, and F.D. Porter. 2020. Abnormal LAMP1 glycosylation may play a role in Niemann-Pick disease, type C pathology. *PloS One.* 15:e0227829. doi:
10.1371/journal.pone.0227829.

Christensen, K.A., J.T. Myers, and J.A. Swanson. 2002. pH-dependent regulation of lysosomal calcium in macrophages. *Journal of Cell Science.* 115:599.

Cystadane® (betaine anhydrous) oral solution. Lebanon, NJ 08833 U.S.A. Recordati Rare Diseases Inc; 2018.

De Duve, C., B.C. Pressman, R. Gianetto, R. Wattiaux, and F. Appelmans. 1955. Tissue fractionation studies. 6. Intracellular distribution patterns of enzymes in rat-liver tissue. *The Biochemical Journal.* 60:604-617. doi: 10.1042/bj0600604.

Demirel, Ö, I. Jan, D. Wolters, J. Blanz, P. Saftig, R. Tampé, and R. Abele. 2012.
The lysosomal polypeptide transporter TAPL is stabilized by interaction with LAMP-1 and LAMP-2. *Journal of Cell Science.* 125:4230-4240. doi:
10.1242/jcs.087346.

Doray, B., P. Ghosh, J. Griffith, H.J. Geuze, and S. Kornfeld. 2002. Cooperation of GGAs and AP-1 in Packaging MPRs at the Trans-Golgi Network. *Science.* 297:1700-1703. doi: 10.1126/science.1075327.

Dorothy F. Bainton. 1981. The Discovery of Lysosomes. *The Journal of Cell Biology.* 91:66s-76s. doi: 10.1083/jcb.91.3.66s.

Dunder, U. 2010. The Application of Enzyme Replacement Therapy in Vitro and in a Mouse Model in Aspartylglycosaminuria. University of Eastern Finland, Kuopio.

Dunder, U., V. Kaartinen, P. Valtonen, E. Väänänen, V.M. Kosma, N. Heisterkamp, J. Groffen, and I. Mononen. 2000. Enzyme replacement therapy in a mouse model of aspartylglycosaminuria. *FASEB Journal : Official Publication of the Federation of American Societies for Experimental Biology.* 14:361-367.
doi: 10.1096/fasebj.14.2.361.

Eskelinen, E., C.K. Schmidt, S. Neu, M. Willenborg, G. Fuertes, N. Salvador, Y. Tanaka, R. Lullmann-Rauch, D. Hartmann, J. Heeren, K. von Figura, E. Knecht, and P. Saftig. 2004. Disturbed Cholesterol Traffic but Normal Proteolytic Function in LAMP-1/LAMP-2 Double-deficient Fibroblasts. *Molecular Biology of the Cell.* 15:3132-3145. doi: 10.1091/mbc.E04-02-0103.

Eskelinen, E., Y. Tanaka, and P. Saftig. 2003. At the acidic edge: emerging functions for lysosomal membrane proteins. *Trends in Cell Biology.* 13:137-145. doi: 10.1016/S0962-8924(03)00005-9.

European Medicines Agency: EMEA/H/C/000678 Cystadane: EPAR. [online] https://www.ema.europa.eu/en/medicines/human/EPAR/cystadane, June 2019

Feng, X., and J. Yang. 2016. Lysosomal Calcium in Neurodegeneration. *Messenger (Los Angeles, Calif. : Print).* 5:56-66. doi: 10.1166/msr.2016.1055.

Fisher, K. J. and J. N. N. Aronson. 1991. Characterization of the mutation responsible for aspartylglucosaminuria in three Finnish patients. Amino acid substitution Cys163----Ser abolishes the activity of lysosomal glycosylasparaginase and its conversion into subunits. Journal of Biological Chemistry. 266:12105.

Fleischer, J.G., R. Schulte, H.H. Tsai, S. Tyagi, A. Ibarra, M.N. Shokhirev, L. Huang, M.W. Hetzer, and S. Navlakha. 2018. Predicting age from the transcriptome of human dermal fibroblasts. Genome Biology. 19:221. doi: 10.1186/s13059-018-1599-6.

Gonzalez-Gomez, I., I. Mononen, N. Heisterkamp, J. Groffen, and V. Kaartinen.
1998. Progressive Neurodegeneration in Aspartylglycosaminuria Mice. *The American Journal of Pathology.* 153:1293-1300. doi: 10.1016/S00029440(10)65674-X.

González-Noriega, A., D.D. Ortega Cuellar, and C. Michalak. 2006. 78 kDa receptor for Man6P-independent lysosomal enzyme targeting: Biosynthetic transport from endoplasmic reticulum to “high-density vesicles”. *Experimental Cell Research.* 312:1065-1078. doi: 10.1016/j.yexcr.2005.12.019.

Grassi, S., E. Chiricozzi, L. Mauri, S. Sonnino, and A. Prinetti. 2019. Sphingolipids and neuronal degeneration in lysosomal storage disorders. *Journal of Neurochemistry.* 148:600-611. doi: 10.1111/jnc.14540.

Greco, M., G. Villani, F. Mazzucchelli, N. Bresolin, S. Papa, and G. Attardi. 2003. Marked aging-related decline in efficiency of oxidative phosphorylation

in human skin fibroblasts. *The FASEB Journal.* 17:1706-1708. doi: 10.1096/fj.02-1009fje.

Grotemeier, A., S. Alers, S.G. Pfisterer, F. Paasch, M. Daubrawa, A. Dieterle, B. Viollet, S. Wesselborg, T. Proikas-Cezanne, and B. Stork. 2010. AMPKindependent induction of autophagy by cytosolic Ca2+ increase. *Cellular Signalling.*22:914-925. doi: 10.1016/j.cellsig.2010.01.015.

Harjunen, E.L., M. Laine, R. Tikkanen, and P. Helenius. 2020. Detailed profile of cognitive dysfunction in children with aspartylglucosaminuria. *Journal of Inherited Metabolic Disease.* 43:318-325. doi: 10.1002/jimd.12159.

Hers, H. 1963. α-Glucosidase deficiency in generalized glycogen-storage disease (Pompe's disease). *Biochemical Journal.* 86:11-16. doi: 10.1042/bj0860011.

Hiesberger, T., S. Hüttler, A. Rohlmann, W. Schneider, K. Sandhoff, and J. Herz. 1998. Cellular uptake of saposin (SAP) precursor and lysosomal delivery by the low density lipoprotein receptor-related protein (LRP). *The EMBO Journal.*17:4617-4625. doi: 10.1093/emboj/17.16.4617.

Hornik, T.C., U. Neniskyte, and G.C. Brown. 2014. Inflammation induces multinucleation of Microglia via PKC inhibition of cytokinesis, generating highly phagocytic multinucleated giant cells. *Journal of Neurochemistry.* 128:650-661. doi: 10.1111/jnc.12477.

Ikonen, E., P. Aula, K. Gron, O. Tollersrud, R. Halila, T. Manninen, A.C. Syvanen, and L. Peltonen. 1991. Spectrum of Mutations in Aspartylglucosaminuria. *Proceedings of the National Academy of Sciences of the United States of America.* 88:11222-11226. doi: 10.1073/pnas.88.24.11222.

Isoniemi, A., M. Hietala, P. Aula, A. Jalanko, and L. Peltonen. 1995. Identification of a novel mutation causing aspartylglucosaminuria reveals a mutation hotspot region in the aspartylglucosaminidase gene. *Human Mutation.* 5:318-326. doi: 10.1002/humu.1380050408.

Jaiswal, J.K., N.W. Andrews, and S.M. Simon. 2002. Membrane Proximal Lysosomes Are the Major Vesicles Responsible for Calcium-Dependent Exocytosis in Nonsecretory Cells. *The Journal of Cell Biology.* 159:625-635. doi: 10.1083/jcb.200208154.

Jalanko, A., K. Tenhunen, C.E. McKinney, M.E. LaMarca, J. Rapola, T. Autti, R. Joensuu, T. Manninen, I. Sipilä, S. Ikonen, J. Riekkinen P, E.I. Ginns, and L. Peltonen. 1998. Mice with an aspartylglucosaminuria mutation similar to humans replicate the pathophysiology in patients. *Human Molecular Genetics.* 7:265-272. doi: 10.1093/hmg/7.2.265.

Kaartinen, V., I. Mononen, I. Gonzales-Gomez, T. Noronkoski, N. Heisterkamp, and J. Groffen. 1998. Phenotypic characterization of mice with targeted disruption of glycosylasparaginase gene: A mouse model for

aspartylglycosaminuria. *J Inherit Metab Dis.* 21:207-209. doi: 10.1023/A:1005387215224.

Kaartinen, V., I. Mononen, J.W. Voncken, T. Noronkoski, I. Gonzalez-Gomez, N. Heisterkamp, and J. Groffen. 1996. A mouse model for the human lysosomal disease aspartylglycosaminuria. *Nature Medicine.* 2:1375-1378. doi: 10.1038/nm1296-1375.

Kaur, G., and A. Lakkaraju. 2018. Early Endosome Morphology in Health and Disease. *Advances in Experimental Medicine and Biology.* 1074:335-343. doi: 10.1007/978-3-319-75402-4_41.

Kelo, E. 2013. Catalytic and Therapeutic Characteristics of Human Recombinant Glycosylasparaginase and Bacterial L-asparaginases. University of Eastern Finland, Kuopio.

Kondratskyi, A., A. Kondratskyi, K. Kondratska, R. Skryma, D.J. Klionsky, D.J. Klionsky, and N. Prevarskaya. 2018. Ion channels in the regulation of autophagy. *Autophagy.* 14:3-21. doi: 10.1080/15548627.2017.1384887.

Lafourcade, C., K. Sobo, S. Kieffer-Jaquinod, J. Garin, and van der Goot, F Gisou. 2008. Regulation of the V-ATPase along the Endocytic Pathway Occurs through Reversible Subunit Association and Membrane Localization. *PloS One.*3:e2758. doi: 10.1371/journal.pone.0002758.

Lefrancois, S., J. Zeng, A.J. Hassan, M. Canuel, and C.R. Morales. 2003. The lysosomal trafficking of sphingolipid activator proteins (SAPs) is mediated by sortilin. *The EMBO Journal.* 22:6430-6437. doi: 10.1093/emboj/cdg629.

Lieberman, A.P., R. Puertollano, N. Raben, S.U. Walkley, A. Ballabio, and S.A. Slaugenhaupt. 2012. Autophagy in Lysosomal Storage Disorders. *Autophagy.* 8:719-730.

Macauley, S.L. 2016. Combination Therapies for Lysosomal Storage Diseases: A Complex Answer to a Simple Problem. *Pediatric Endocrinology Reviews : PER.* 13 Suppl 1:639-648.

Maxfield, F.R., and D.J. Yamashiro. 1987. Endosome acidification and the pathways of receptor-mediated endocytosis. *Advances in Experimental Medicine and Biology.* 225:189-198.

McCormack, A.L., I. Mononen, V. Kaartinen, and J.R. Yates III. 1995. Localization of the Disulfide Bond Involved in Post-translational Processing of Glycosylasparaginase and Disrupted by a Mutation in the Finnish-type Aspartylglycosaminuria. *Journal of Biological Chemistry.* 270:3212-3215. doi: 10.1074/jbc.270.7.3212.

McGill University Health Centre/Research Institute of the McGill University Health Centre. Betaine and Peroxisome Biogenesis Disorders. Available from: https://clinicaltrials.gov/ct2/show/NCT01838941. NLM identifier: NCT01838941. Accessed March 23, 2020.

Medina, D., A. Fraldi, V. Bouche, F. Annunziata, G. Mansueto, C. Spampanato, C. Puri, A. Pignata, J. Martina, M. Sardiello, M. Palmieri, R. Polishchuk, R. Puertollano, and A. Ballabio. 2011. Transcriptional Activation of Lysosomal Exocytosis Promotes Cellular Clearance. *Developmental Cell.* 21:421-430. doi: 10.1016/j.devcel.2011.07.016.

Medina, D.L., S. Di Paola, I. Peluso, A. Armani, D. Stefani, R. Venditti, S. Montefusco, A. Scotto-Rosato, C. Prezioso, A. Forrester, C. Settembre, W. Wang, Q. Gao, H. Xu, M. Sandri, R. Rizzuto, M.A. Matteis, and A. Ballabio. 2015. Lysosomal calcium signaling regulates autophagy via calcineurin and TFEB. *Nature Cell Biology.* 17:288-299. doi: 10.1038/ncb3114.

Meikle, P.J., J.J. Hopwood, A.E. Clague, and W.F. Carey. 1999. Prevalence of Lysosomal Storage Disorders. *Jama.*281:249-254. doi: 10.1001/jama.281.3.249.

Mizushima, N., T. Yoshimori, and B. Levine. 2010. Methods in Mammalian Autophagy Research. *Cell.* 140:313-326. doi: 10.1016/j.cell.2010.01.028.

Mononen, I., N. Heisterkamp, V. Kaartinen, J. C. Williams, J. R. Yates, P. R. Griffin, L. E. Hood, and J. Groffen. 1991. Aspartylglycosaminuria in the Finnish Population: Identification of Two Point Mutations in the Heavy Chain of Glycoasparaginase. *Proceedings of the National Academy of Sciences of the United States of America.* 88:2941-2945. doi: 10.1073/pnas.88.7.2941.

Mononen, I., N. Heisterkamp, U. Dunder, E.L. Romppanen, T. Noronkoski, I. Kuronen, and J. Groffen. 1995. Recombinant glycosylasparaginase and in vitro correction of aspartylglycosaminuria. *The FASEB Journal.* 9:428-433. doi: 10.1096/fasebj.9.5.7896015.

Mononen, I., V. Kaartinen, and T. Mononen. 1988. Laboratory detection of aspartylglucosaminuria. *Scand J Clin Lab Invest.* 48:7-11.

Mononen, I.T., V.M. Kaartinen, and J.C. Williams. 1993. A Fluorometric Assay for Glycosylasparaginase Activity and Detection of Aspartylglycosaminuria. *Analytical Biochemistry.* 208:372-374. doi: 10.1006/abio.1993.1063.

Näntö-Salonen, K., and R. Penttinen. 1982. Metabolism of collagen in aspartylglycosaminuria: Decreased synthesis by cultured fibroblasts. *Journal of Inherited Metabolic Disease.* 5:197-203. doi: 10.1007/BF02179141.

Nishino, I., J. Fu, K. Tanji, T. Yamada, S. Shimojo, T. Koori, M. Mora, J.E. Riggs,
S.J. Oh, Y. Koga, C.M. Sue, A. Yamamoto, N. Murakami, S. Shanske, E. Byrne, E. Bonilla, I. Nonaka, S. DiMauro, and M. Hirano. 2000. Primary LAMP-2 deficiency causes X-linked vacuolar cardiomyopathy and myopathy (Danon disease). *Nature.* 406:906-910. doi: 10.1038/35022604.

Norio, R. 2003. The Finnish disease heritage III: the individual diseases. *Hum Genet.* 112:470-526. doi: 10.1007/s00439-002-0877-1.

Ohkuma, S., Y.Moriyama, and T. Takano. 1982. Identification and

Characterization of a Proton Pump on Lysosomes by Fluorescein IsothiocyanateDextran Fluorescence. *Proceedings of the National Academy of Sciences of the United States of America.* 79:2758-2762. doi: 10.1073/pnas.79.9.2758.

Oinonen, C., R. Tikkanen, J. Rouvinen, and L. Peltonen. 1995. Threedimensional structure of human lysosomal aspartylglucosaminidase. *Nature Structural Biology.* 2:1102-1108. doi: 10.1038/nsb1295-1102.

Palmieri, M., S. Impey, H. Kang, A. di Ronza, C. Pelz, M. Sardiello, and A. Ballabio. 2011. Characterization of the CLEAR network reveals an integrated control of cellular clearance pathways. *Human Molecular Genetics.* 20:38523866. doi: 10.1093/hmg/ddr306.

Parkinson-Lawrence, E.J., T. Shandala, M. Prodoehl, R. Plew, G. Borlace, and D.A. Brooks. 2010. Lysosomal storage disease : revealing lysosomal function and physiology. *Physiology.* 25:102–115.

Paul R. Pryor, Barbara M. Mullock, Nicholas A. Bright, Sally R. Gray, and J. Paul Luzio. 2000. The Role of Intraorganellar Ca2+in Late Endosome-Lysosome Heterotypic Fusion and in the Reformation of Lysosomes from Hybrid Organelles. *The Journal of Cell Biology.* 149:1053-1062. doi: 10.1083/jcb.149.5.1053.

Platt, F.M. 2018. Emptying the stores: lysosomal diseases and therapeutic strategies. *Nature Reviews Drug Discovery.* 17:133-150. doi: 10.1038/nrd.2017.214.

Ravikumar, B., C. Vacher, Z. Berger, J.E. Davies, L. Shouqing, L.G. Oroz, F. Scaravilli, D.F. Easton, R. Duden, C.J. O'Kane, and D.C. Rubinstein. 2004. Inhibition of mTOR induces autophagy and reduces toxicity of polyglutamine expansions in fly and mouse models of Huntington disease. *Nature Genetics.* 36:585-595. doi: 10.1038/ng1362.

Ravikumar, B., S. Sarkar, J.E. Davies, M. Futter, M. Garcia-Arencibia, Z.W. Green-Thompson, M. Jimenez-Sanchez, V.I. Korolchuk, M. Lichtenberg, S Luo,
D.C.O. Massey, F.M. Menzies, K. Moreau, U. Narayanan, M. Renna, F.H. Siddiqi, B.R. Underwood, A.R. Winslow, and D.C. Rubinsztein. 2010. Regulation of Mammalian Autophagy in Physiology and Pathophysiology. *Physiological Reviews.* 90:1383-1435. doi: 10.1152/physrev.00030.2009.

Reczek, D., M. Schwake, J. Schröder, H. Hughes, J. Blanz, X. Jin, W. Brondyk, S. Van Patten, T. Edmunds, and P. Saftig. 2007. LIMP-2 Is a Receptor for Lysosomal Mannose-6-Phosphate-Independent Targeting of β-Glucocerebrosidase. *Cell.* 131:770-783. doi: 10.1016/j.cell.2007.10.018.

Reitman, M.L., and S. Kornfeld. 1981. Lysosomal Enzyme Targeting. *The Journal of Biological Chemistry.* 256:11977-11980.

Riikonen, A., R. Tikkanen, A. Jalanko, and L. Peltonen. 1995. Immediate interaction between the nascent subunits and two conserved amino acids

Trp34 and Thr206 are needed for the catalytic activity of aspartylglucosaminidase. *The Journal of Biological Chemistry.* 270:4903-4907.

Rodríguez, A., P. Webster, J. Ortego, and N.W. Andrews. 1997. Lysosomes Behave as Ca2+-Regulated Exocytic Vesicles in Fibroblasts and Epithelial Cells. *The Journal of Cell Biology.* 137:93-104. doi: 10.1083/jcb.137.1.93.

Rohrer, J., and R. Kornfeld. 2001. Lysosomal Hydrolase Mannose 6-Phosphate Uncovering Enzyme Resides in the trans-Golgi Network. *Molecular Biology of the Cell.* 12:1623-1631. doi: 10.1091/mbc.12.6.1623.

Ruivo, R., C. Anne, C. Sagné, and B. Gasnier. 2009. Molecular and cellular basis of lysosomal transmembrane protein dysfunction. *BBA - Molecular Cell Research.* 1793:636-649. doi: 10.1016/j.bbamcr.2008.12.008.

Saarela, J., C. Oinonen, A. Jalanko, J. Rouvinen, And L. Peltonen. 2004. Autoproteolytic activation of human aspartylglucosaminidase. *Biochemical Journal.* 378:363-371. doi: 10.1042/bj20031496.

Saftig, P., and J. Klumperman. 2009. Lysosome biogenesis and lysosomal membrane proteins: trafficking meets function. *Nature Reviews Molecular Cell Biology.* 10:623-635. doi: 10.1038/nrm2745.

Samarani, M., N. Loberto, G. Soldà, L. Straniero, R. Asselta, S. Duga, G. Lunghi, F.A. Zucca, L. Mauri, M.G. Ciampa, D. Schiumarini, R. Bassi, P. Giussani, E. Chiricozzi, A. Prinetti, M. Aureli, and S. Sonnino. 2018. A lysosome–plasma membrane–sphingolipid axis linking lysosomal storage to cell growth arrest. *FASEB Journal : Official Publication of the Federation of American Societies for Experimental Biology.* 32:5685-5702. doi: 10.1096/fj.201701512RR.

Samie, M.A., and H. Xu. 2014. Lysosomal exocytosis and lipid storage disorders. *Journal of Lipid Research.* 55:995-1009. doi: 10.1194/jlr.R046896.

Sands, M.S., and B.L. Davidson. 2006. Gene Therapy for Lysosomal Storage Diseases. *Molecular Therapy.* 13:839-849. doi: 10.1016/j.ymthe.2006.01.006.

Sapmaz, A., I. Berlin, E. Bos, R.H. Wijdeven, H. Janssen, R. Konietzny, J.J. Akkermans, A.E. Erson-Bensan, R.I. Koning, B.M. Kessler, J. Neefjes, and H. Ovaa. 2019. USP32 regulates late endosomal transport and recycling through deubiquitylation of Rab7. *Nature Communications.* 10:1454-18. doi: 10.1038/s41467-019-09437-x.

Sardiello, M., M. Palmieri, A. di Ronza, D.L. Medina, M. Valenza, V.A. Gennarino, C. Di Malta, F. Donaudy, V. Embrione, R.S. Polishchuk, S. Banfi, G. Parenti, E. Cattaneo, and A. Ballabio. 2009. A Gene Network Regulating Lysosomal Biogenesis and Function. *Science.* 325:473-477. doi: 10.1126/science.1174447.

Schnaar, R.L. 2016. Gangliosides of the Vertebrate Nervous System. *Journal of Molecular Biology.* 428:3325-3336. doi: 10.1016/j.jmb.2016.05.020.

Schultz, M.L., L. Tecedor, M. Chang, and B.L. Davidson. 2011. Clarifying lysosomal storage diseases. *Trends in Neurosciences.* 34:401-410. doi: 10.1016/j.tins.2011.05.006.

Schulze, H., and K. Sandhoff. 2011. Lysosomal Lipid Storage Diseases. *Cold Spring Harbor Perspectives in Biology.* 3. doi: 10.1101/cshperspect.a004804.

Schwake, M., B. Schröder, and P. Saftig. 2013. Lysosomal Membrane Proteins and Their Central Role in Physiology. *Traffic.* 14:739-748. doi: 10.1111/tra.12056.

Settembre, C., and A. Ballabio. 2011. TFEB regulates autophagy: An integrated coordination of cellular degradation and recycling processes. *Autophagy.* 7:1379-1381. doi: 10.4161/auto.7.11.17166.

Settembre, C., C.D. Malta, V.A. Polito, M.G. Arencibia, F. Vetrini, S. Erdin, S.U. Erdin, T. Huynh, D. Medina, P. Colella, M. Sardiello, D.C. Rubinsztein, and A. Ballabio. 2011. TFEB Links Autophagy to Lysosomal Biogenesis. *Science.* 332:1429-1433. doi: 10.1126/science.1204592.

Song, W., F. Wang, P. Lotfi, M. Sardiello, and L. Segatori. 2014. 2-Hydroxypropyl-β-cyclodextrin promotes transcription factor EB-mediated activation of autophagy: implications for therapy. *The Journal of Biological Chemistry.* 289:10211-10222. doi: 10.1074/jbc.M113.506246.

Spampanato, C., E. Feeney, L. Li, M. Cardone, J. Lim, F. Annunziata, H. Zare, R. Polishchuk, R. Puertollano, G. Parenti, A. Ballabio, and N. Raben. 2013. Transcription factor EB (TFEB) is a new therapeutic target for Pompe disease. *EMBO Molecular Medicine.* 5:691-706. doi: 10.1002/emmm.201202176.

Stoorvogel, W., G.J. Strous, H.J. Geuze, V. Oorschot, and A.L. Schwartzt. 1991. Late endosomes derive from early endosomes by maturation. *Cell.* 65:417-427. doi: 10.1016/0092-8674(91)90459-C.

Sugita, S., R. Munechika, and M. Nakamura. 2019. Multinucleation of Incubated Cells and Their Morphological Differences Compared to Mononuclear Cells. *Micromachines.* 10:156. doi: 10.3390/mi10020156.

Sun, M., E. Goldin, S. Stahl, J.L. Falardeau, J.C. Kennedy, J. Acierno J S, C. Bove, C.R. Kaneski, J. Nagle, M.C. Bromley, M. Colman, R. Schiffmann, and S.A. Slaugenhaupt. 2000. Mucolipidosis type IV is caused by mutations in a gene encoding a novel transient receptor potential channel. *Human Molecular Genetics.* 9:2471-2478. doi: 10.1093/hmg/9.17.2471.

Tenhunen, K., A. Uusitalo, T. Autti, R. Joensuu, M. Kettunen, R. Kauppinen, S. Ikonen, M. Lamarca, M. Haltia, E. Ginns, A. Jalanko, and L. Peltonen. 1998. Monitoring the CNS Pathology in Aspartylglucosaminuria Mice. *Journal of Neuropathology and Experimental Neurology.* 57:1154-1163. doi: 10.1097/00005072-199812000-00007.

Tikkanen, R., A. Riikonen, C. Oinonen, R. Rouvinen, and L. Peltonen. 1996. Functional analyses of active site residues of human lysosomal aspartylglucosaminidase: implications for catalytic mechanism and autocatalytic activation. *The EMBO Journal.* 15:2954-2960. doi: 10.1002/j.1460-2075.1996.tb00658.x.

Tokola, A.M., L.E. Åberg, and T.H. Autti. 2015. Brain MRI findings in aspartylglucosaminuria. *Journal of Neuroradiology.* 42:345-357. doi: 10.1016/j.neurad.2015.03.003.

Trombetta, E.S., M. Ebersold, W. Garrett, M. Pypaert, and I. Mellman. 2003.Activation of Lysosomal Function During Dendritic Cell Maturation. *Science.* 299:1400-1403. doi: 10.1126/science.1080106.

Uniprot.org/P20933. The UniProt Consortium UniProt: the universal protein knowledgebase. Nucleic Acids Res. 46: 2699 (2018)

Wang, Z., C. Yang, J. Liu, B. Chun-Kit Tong, Z. Zhu, S. Malampati, S. Gopalkrishnashetty Sreenivasmurthy, K. Cheung, A. Iyaswamy, C. Su, J. Lu, J. Song, and M. Li. 2020. A Curcumin Derivative Activates TFEB and Protects Against Parkinsonian Neurotoxicity in Vitro. *International Journal of Molecular Sciences.* 21:1515. doi: 10.3390/ijms21041515.

Yamamoto, A., Y. Tagawa, T. Yoshimori, Y. Moriyama, R. Masaki, and Y. Tashiro. 1998. Bafilomycin A1 Prevents Maturation of Autophagic Vacuoles by Inhibiting Fusion between Autophagosomes and Lysosomes in Rat Hepatoma Cell Line, H-4-II-E Cells. *Cell Structure and Function.* 23:33-42. doi: 10.1247/csf.23.33.

Yuan, Y., L. Li, L. Zhu, F. Liu, X. Tang, G. Liao, J. Liu, J. Cheng, Y. Chen, and Y. Lu. 2020. Mesenchymal stem cells elicit macrophages into M2 phenotype via improving transcription factor EB-mediated autophagy to alleviate diabetic nephropathy. *Stem Cells.* doi: 10.1002/stem.3144.

Zhuang, X., S. Wang, Y. Tan, J. Song, Z. Zhu, Z. Wang, M. Wu, C. Cai, Z. Huang, J. Tan, H. Su, M. Li, and J. Lu. 2020. Pharmacological enhancement of TFEBmediated autophagy alleviated neuronal death in oxidative stress-induced Parkinson's disease models. *Cell Death & Disease.* 11:128. doi: 10.1038/s41419-020-2322-6.